FORMATION OF CONCENTRATION GRADIENTS OF MONOCYTE CHEMOATTRACTANT PROTEIN-1 IN A COLLAGEN MATRIX

By

KRISADA LEEMASAWATDIGUL

Bachelor of Engineering in Chemical Engineering

Chulalongkorn University

Bangkok, Thailand

2007

Submitted to the Faculty of the
Graduate College of the
Oklahoma State University
in partial fulfillment of
the requirements for
the Degree of
MASTER OF SCIENCE
July, 2010

FORMATION OF CONCENTRATION GRADIENTS

OF MONOCYTE CHEMOATTRACTANT

PROTEIN-1 IN A COLLAGEN MATRIX

Thesis Approved:

Dr. Heather Fahlenkamp

Thesis Adviser

Dr. Sundararajan V. Madihally

Dr. Joshua D. Ramsey

Dr. Mark E. Payton

Dean of the Graduate College

ACKNOWLEDGMENTS

I would like to express my sincere gratitude to my advisor, Dr. Heather Fahlenkamp, for introducing me to this interesting field of study, as well as giving me all of the advices and suggestions throughout every step of this research project. By working under her supervision, I have learnt so many things, all of which I truly believe will be very beneficial to me when working in the professional level. Without her guidance, this research project could have never been this successful. I am also grateful to Dr. Sundar Madihally and Dr. Josh Ramsey for being my committee members and providing valuable comments and recommendations to improve this thesis.

I would like to thank the department staffs, Eileen, Mindy, Carolyn, and Melissa, for their help in administrative matters, and Shelley for her help as a lab manager. I thank my lab colleagues, Subuola and Munish, for their help. I thank all of my friends in the Thai Student Association for making my past two years at OSU a very good time. I am also deeply thankful to Kornkarn for always supporting me on every aspect, including suggestions on writing this thesis and preparing a presentation for my thesis defense.

Mostly importantly, I would like to thank my family for all of their unconditional love and support, especially my dad, who not only inspired me to study in the field of Chemical Engineering, but also encouraged me to study further to the graduate level. To him, I dedicate this thesis.

TABLE OF CONTENTS

Chapter Page

LIST OF TABLES

Table Page

LIST OF FIGURES

Figure Page

Figure Page

CHAPTER I

INTRODUCTION

Cardiovascular disease (CVD) is a major health problem in many developed countries. CVD is the leading cause of death in both Europe and the United States. Each year in Europe, more than 4.3 million people die because of CVD, accounting for almost half of the total deaths in the region [1]. In the United States, about one third (830,000 deaths) of the overall mortalities in 2006 were caused by CVD – according to data from National Center for Health Statistics, and over 80 million adults are believed to suffer some form(s) of CVD [2]. The economic burden of CVD, which is estimated from healthcare expenditure and the lost of productivity due to disability or death, for the United States alone is expected to be more than $503 billion in 2010 [3].

Atherosclerosis is the primary cause of CVD, including myocardial infarction, or heart attack, and stroke. Atherosclerosis is a progressive disease characterized by the buildup of lipid substances, immune cells, and fibrous elements in the inner lining of large arteries (**Figure 1.1**) [4, 5]. The buildup is called plaque, which can grow large enough to significantly reduce blood flow in an artery. However, more adverse clinical complications can occur when the plaque ruptures and causes a blood clot to form in the vessel. The blood clot, or thrombus, can block blood flow and results in the loss of blood

supply to vital organs. If the thrombus occurs in arteries that lead to the arms or legs, it can cause gangrene – the death of soft tissue in those body parts. If the thrombus occurs in an artery leading to the heart or brain, it may cause a heart attack or stroke, respectively.

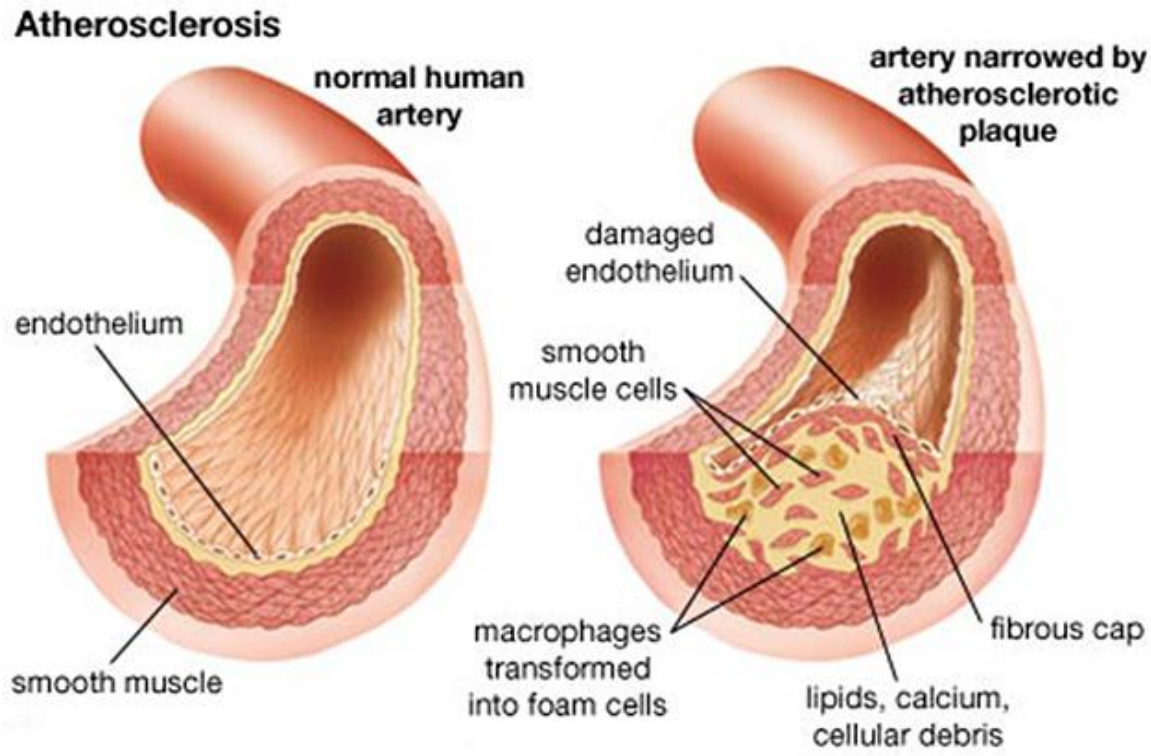

Figure 1.1 Comparison between normal artery and one with atherosclerotic plaque.

(*Picture source: http://www.tappmedical.com/atherosclerosis.htm*)

In the past, atherosclerosis was linked to cholesterol and was believed to be caused by an injury to the arterial wall. Due to advances in vascular biology, atherosclerosis is now viewed as an inflammatory disease, as suggested by Russell Ross [6]. Risk factors associated with the disease include, but not limit to, high blood pressure (hypertension), cigarette smoking, diabetes, and high cholesterol (hypercholesterolemia)

[4, 7, 8]. The initiation of the atherosclerotic lesion begins with the deposition of low-density lipoprotein (LDL), which is a carrier of insoluble lipids, such as cholesterol in the water-based bloodstream, within the extracellular matrix (ECM) underneath the endothelial layer. (Endothelial layer or endothelium is a single layer of cells that represent the inner most lining of an artery as displayed in **Figure 1.1**.) The deposited LDL, if modified by oxidation, glycation (in case of diabetes), or other mechanisms, stimulates neighboring endothelial cells to send out inflammatory signals to recruit leukocytes or white blood cells into the area. Modified LDL itself possesses an ability to attract the migration of leukocytes into the injured site as well [9]. Once leukocytes are localized in the subendothelial matrix, they response to the signals sent from the stimulated endothelial cells in various ways. For monocytes, they differentiate into macrophages, which can subsequently engorge surrounding modified LDL and transform into foam cells. These foam cells can also produce inflammatory signals, resulting in the extended number of leukocytes being recruited into the area. If the injurious agent like modified LDL is still present, the whole process will continue and lead to the development of an atherosclerotic lesion.

One of the important events during the initiation of atherosclerosis is the transendothelial migration of leukocytes. Involved in this multi-step process are cellular adhesion molecules (CAMs) and chemotactic cytokines (chemokines). CAMs are proteins expressed on the surface of cells and are involved with intercellular binding. The role of CAMs in atherosclerosis is to capture of leukocytes from the bloodstream onto endothelium and the transmigration of leukocytes into the ECM [10, 11]. Chemokines are small proteins that are potent activators and attractants to leukocytes. In

atherosclerosis, the recruitment of leukocytes and their successive transmigration are assisted by this group of proteins [11, 12]. Because both CAMs and chemokines are critical participants in the inflammatory process associated with atherosclerosis, they are suggested to be potent therapeutic targets for the treatment and prevention of this disease. However, a better understanding of the underlying mechanisms between these two groups of proteins and the progression of this disease is required in order to develop highly specific therapeutic strategies.

In our laboratory, an advance three-dimensional (3D) *in vitro* vascular tissue model was introduced as a tool to study cellular mechanisms involved in the early stages of atherosclerosis. The major advantage of this 3D tissue model, compared to traditional cell culture systems used in this field of study, is the addition of collagen matrix, which mimics the ECM below the endothelial layer (**Figure 1.2**). Unlike the traditional cell culture systems, in which soluble factors that are secreted from endothelial cells dissolve quickly into the surrounding medium, the collagen matrix of the 3D tissue model provides a supplementary space that allows the gradients of the soluble factors to be created. The gradients formed in the collagen matrix should mimic those formed *in vivo* in the ECM, which are responsible for the control of many cellular mechanisms. For example, gradients of chemokines are known to have migratory effect on leukocytes [13-15]. Apart from the gradients of soluble factors, when focusing on the transmigration of monocytes, the collagen matrix of the 3D tissue model also provides an area for monocytes to localize and differentiate into macrophages after the transendothelial migration. This latter property of the 3D tissue model makes it applicable as a testing device for therapeutics of atherosclerosis in the future.

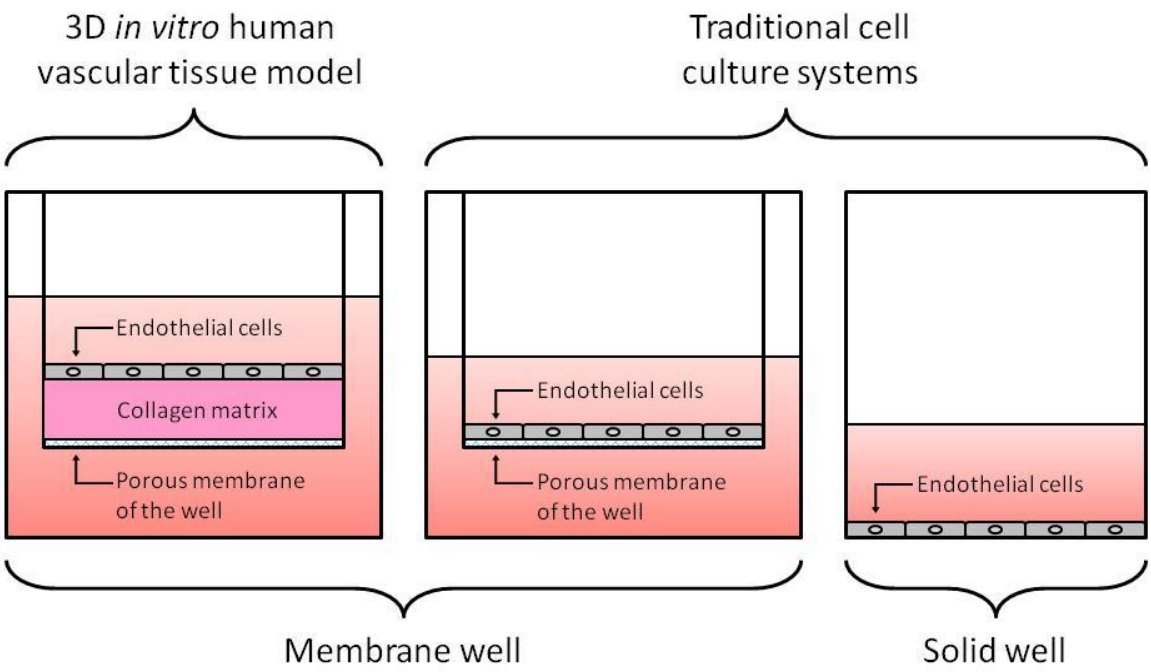

Figure 1.2 Comparison between traditional cell culture systems and 3D *in vitro* human vascular tissue model

The goal of our laboratory in using the 3D tissue model is to characterize CAMs and chemokines that are key in the transmigration of monocytes into atherosclerotic-lesion prone areas. This migration process is crucial in the early stage of atherosclerosis. The main focus of this goal is to determine whether the capturing and successive migration across the endothelium of monocytes are controlled by CAMs alone, or a gradient of monocyte chemoattractant protein-1 (MCP-1) – a secreted chemokine that possesses an ability to attract monocytes – also takes part in these migration steps. As an initial step to fulfill this goal, the quantification of the MCP-1 concentration gradient in the collagen matrix of the 3D tissue model is required. Presently, there is no available technique that can be used to quantify such a gradient inside the collagen matrix directly. The objective of this research project is to develop a mathematical model that describes

both the transport and kinetic behaviors of MCP-1 in the collagen matrix of the 3D tissue model. Results from this mathematical model were aimed to provide an estimation of the concentration gradient of MCP-1 in the collagen matrix.

Main objective:

- In summary, this project focuses on the development of a mathematical model that describes the formation of MCP-1 concentration gradient in the collagen matrix. To develop the mathematical model, it is important to understand the transport and kinetics behaviors of MCP-1 in the matrix. For the kinetics aspect, it was initially hypothesized that MCP-1 is stable at standard cell culture conditions (37°C in humidified atmosphere of 5% CO_2 and 95% air) and there is no binding reaction between MCP-1 and collagen in the matrix. Experiments were done to test this hypothesis.

Sub objectives:

- Determine the stability of MCP-1 at standard cell culture conditions.
- Examine the binding reaction between MCP-1 and collagen in the matrix.

CHAPTER II

DEVELOPMENT OF A MATHEMATICAL MODEL TO DESCRIBE THE TRANSPORT OF MCP-1 THROUGH A THREE-DIMENSIONAL COLLAGEN MATRIX

Atherosclerosis is an inflammatory disease [6], which is characterized by endothelial dysfunction, inflammation, extracellular matrix (ECM) remodeling, and smooth muscle cell migration [16]. The steps in atherosclerosis plaque formation begin with the subendothelial accumulation of lipid substances, followed by the adhesion of monocytes and lymphocytes to endothelial cells and their subsequent migration across the endothelial layer to the ECM [17, 18]. Once localized in the subendothelial space, monocytes differentiate into active macrophages and form foam cells by interacting with oxidized low-density lipoprotein (Ox-LDL) and consuming lipid substances [6, 19]. The foam cells continue to produce inflammatory signals, which results in more monocyte recruitment to the area and the development of an atherosclerosis lesion [19].

There are many bioactive molecules associated in the initiation of atherosclerosis plaque. E-selectin and P- selectin, along with endothelial adhesion molecules, intercellular adhesion molecule-1 (ICAM-1) and vascular cell adhesion molecule-1 (VCAM-1), are found to mediate the adhesion process of leukocytes onto the endothelial

surface [20-22]. Monocyte chemoattractant protein-1 (MCP-1) is another bioactive molecule that is thought to play an important role in the formation of an early atherosclerosis lesion. The function of MCP-1 in atherosclerosis includes the attraction of monocytes to the subendothelial matrix. Studies show that the level of MCP-1 is upregulated in human atherosclerosis lesions [23, 24], and the lack of MCP-1 in a mouse model reduces macrophage formation [25, 26]. These experimental studies suggest that MCP-1 may be a potent therapeutic target for this disease.

Monocyte trafficking across the endothelial layer is believed to be mediated by an MCP-1 concentration gradient. This concept is supported by many studies [14, 15], including the work of Randolph and Furie [13], which illustrates *in vitro* that the transendothelial migration of monocytes depends on the soluble concentration gradient of MCP-1 across the endothelial layer. It was also shown in this latter study that MCP-1 is equally secreted from apical and basal sides of stimulated endothelial cells [13]. This finding combined with the fact that MCP-1 is secreted in a soluble form suggests that *in vivo*, where the blood flow in the vascular could prevent the formation of a MCP-1 concentration gradient in the lumen side, the concentration gradient of MCP-1 may be formed within the ECM via the diffusion of MCP-1 secreted from the basal of the endothelial layer [27]. However, information characterizing the effect of the diffusive gradient of MCP-1 in the subendothelial matrix to monocyte transmigration is still lacking. The limitation is due to the difficulty in quantitatively determining the concentration of MCP-1 in the matrix.

In the present study, we introduced the application of a 3D *in vitro* vascular tissue model [28] to investigate the formation of a diffusive gradient of MCP-1. In contrast to a

traditional 2D cell culture system, where MCP-1 that is secreted from a monolayer of endothelial cells dissolves quickly into the surrounding media, this 3D tissue model provides a layer of collagen matrix in which the diffusive gradient of secreted MCP-1 can be formed. The main objective of this paper is to develop a mathematical model that can determine MCP-1 concentration gradient within the collagen matrix. The mathematical model describes both diffusive and kinetic behaviors of MCP-1 in the matrix. The stability of MCP-1 under standard conditions and the binding reaction between MCP-1 and the collagen matrix were investigated to describe the behavior of MCP-1 in the matrix. In order to focus just on the behavior of MCP-1 in the collagen matrix, the release of MCP-1 by endothelial cells is not covered in this paper. Instead, MCP-1 was added to the top reservoir of the 3D tissue model as an initial source. For future work, endothelial cells will be included to the tissue model and the source term of the current mathematical model will be updated.

Initial assumptions:

Figure 2.1 shows the schematic diagram of the 3D *in vitro* vascular tissue model without cells. The tissue model was constructed by adding collagen solution into a membrane well. The cross-sectional area of the insert of the membrane well used in this study is 33 mm^2. The membrane material is polystyrene with a pore size and thickness of 3 μm and 10 μm, respectively. The mathematical model to determine MCP-1 concentration gradient in the collagen matrix was developed based on the equation of continuity. Several assumptions were applied to simplify the equation. First, the migration of MCP-1 through the collagen matrix in the 3D vascular tissue model is assumed to be due to diffusive mass transfer only (no convective mass transfer occurred

in the system). Second, because the focus of this study is on the gradient of MCP-1 in the perpendicular direction from the endothelial layer, or the top surface of the collagen matrix, the diffusion is assumed to be only in such direction (z-direction). Third, the effect of MCP-1 mass transfer across the membrane that supports the collagen matrix is assumed to be insignificant compared to mass transport across the collagen matrix, because the thickness of the membrane is significantly less than that of the collagen matrix and the pore size of the membrane is significantly larger than the size of the MCP-1 molecule. The wall effect within the membrane well and the curvature of the top surface of the collagen matrix are also neglected.

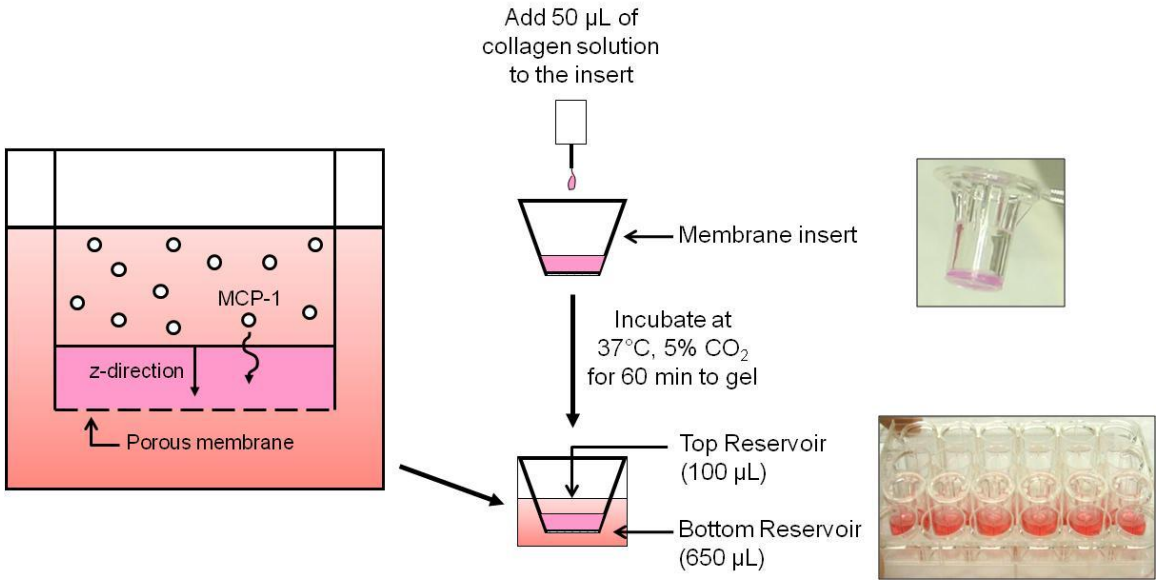

Figure 2.1 Schematic diagram of the 3D *in vitro* vascular tissue model without cells. A collagen matrix is formed within the well of a 24-well Transwell® plate.

By applying these assumptions to the equation of continuity, the main equation of the model becomes

$$\frac{\partial C_M(z,t)}{\partial t} = D_{M|C}\left(\frac{\partial^2 C_M(z,t)}{\partial z^2}\right) + R_M(z,t) \quad (2.1)$$

where C_M is the molar concentration of MCP-1, z is the distance from the top surface of the collagen matrix, t is time, $D_{M|C}$ is the diffusivity coefficient of MCP-1 in the matrix, which is assumed to be constant, and R_M is a rate term.

The rate term describes the rate of MCP-1 that is reacted or consumed in the collagen matrix, and was still unknown at this point. We hypothesized that MCP-1 was stable under standard culture conditions (37°C, and humidified atmosphere of 5% CO_2 and 95% air), and it did not bind with the collagen matrix. The hypothesis was tested experimentally.

Materials and methods:

Materials

Recombinant human MCP-1 was purchased from R&D Systems (Minneapolis, MN). Dulbecco's phosphate-buffered saline (D-PBS), Medium 199, and penicillin-streptomycin-glutamine (PSG) solution were purchased from Invitrogen (Carlsbard, CA). Fetal bovine serum (FBS) was purchased from Hyclone (Logan, UT). PureCol® collagen (97% Type 1 collagen) was purchased from Advanced BioMatrix (San Diego, CA). Sodium hydroxide was purchased from VWR (West Chester, PA). Corning Transwell® permeable supports and Tween® 20 were purchased from Fisher Scientific (Pittsburgh, PA). Bovine serum albumin (BSA) was purchased from Sigma-Aldrich (St.

Louis, MO). BD OptEIA™ Human MCP-1 enzyme-linked immunosorbent assay (ELISA) set was purchased from BD Biosciences (San Jose, CA).

MCP-1 stability test

Complete medium (Medium 199 with 10 vol% FBS and 1 vol% PSG) was used to prepare MCP-1 solutions at the following concentrations: 0.25, 5, 15, 25, and 50 ng/mL. The MCP-1 solutions were incubated at standard conditions for 24 hours. Samples were taken from the solutions every six hours during the incubation and stored at -81°C, until ready for analysis. The level of MCP-1 in the samples was determined by ELISA.

Development of the 3D in vitro vascular tissue model without cells

The main procedure to construct the 3D vascular tissue model in this study is similar to the one described previously [28], but a 24-well Transwell® plate is used instead of a 48-well plate and no endothelial cells were seeded on top of collagen matrix. Briefly, collagen matrix was prepared by adding 50 µL of collagen solution containing 57.1 vol% PureCol® collagen (3 mg/mL), 7.14 vol% Medium 199, and 35.7 vol% 0.1 M sodium hydroxide to each insert of a Transwell® plate. The plate was incubated at standard conditions for 60 minutes for the collagen to gel. Prior to testing, complete medium was added to the top and the bottom reservoirs of the plate, and the plate was incubated at standard conditions for four hours to equilibrate the collagen gels.

MCP-1 binding reaction test

Complete medium containing one of the following concentrations of MCP-1 was selected as a source of MCP-1 and added to the top reservoir of the complete 3D vascular

tissue model without cells: 0.25, 5, 15, 25, or 50 ng/mL. The bottom reservoir was filled with complete medium. The 3D vascular tissue model was incubated at standard conditions for 24 hours to allow MCP-1 to diffuse from the top reservoir through the collagen matrix to the bottom reservoir. During the incubation, samples were taken from both the top and the bottom reservoirs and were stored at -81°C, until ready for analysis. The MCP-1 concentration of the samples was analyzed by ELISA and was used to determine the binding reaction between MCP-1 and the collagen matrix.

MCP-1 ELISA

ELISA was performed according to the manufacturer's instructions, except that complete medium was used as diluents for standards and samples instead of Assay Diluent. The absorbance was measured with an Emax precision microplate reader (Molecular Devices, Sunnyvale, CA) at the 450 nm wavelength subtracted by the 540 nm reference wavelength. MCP-1 concentrations were determined by comparing absorbance readings to those from known standard concentrations developed from the same assay.

Statistical analysis

MCP-1 concentrations are expressed as mean ± SD of three samples or more. Student's *t* test was used to determine significant differences in the MCP-1 stability test results, and the estimated MCP-1 concentration in collagen matrix results. A value of $p < 0.05$ was considered significant. Absolute-average-percentage deviation (%AAD) was used to compare the difference between experimental results and results from the mathematical model.

Experimental results:

MCP-1 stability test

Initially, it was assumed that MCP-1 is stable at standard conditions. To test this assumption, complete medium containing various concentrations of MCP-1 was incubated at standard conditions for 24 hours. Samples were collected from the complete medium during that time and analyzed for the concentration of MCP-1. The results in **Figure 2.2** show that the concentrations of MCP-1 at the later time points (12, 18, and 24 hours) do not change significantly when compared to the concentrations at the first time point (6 hours) of samples in the same group. Thus, we concluded that MCP-1 is stable at standard conditions for at least 24 hours.

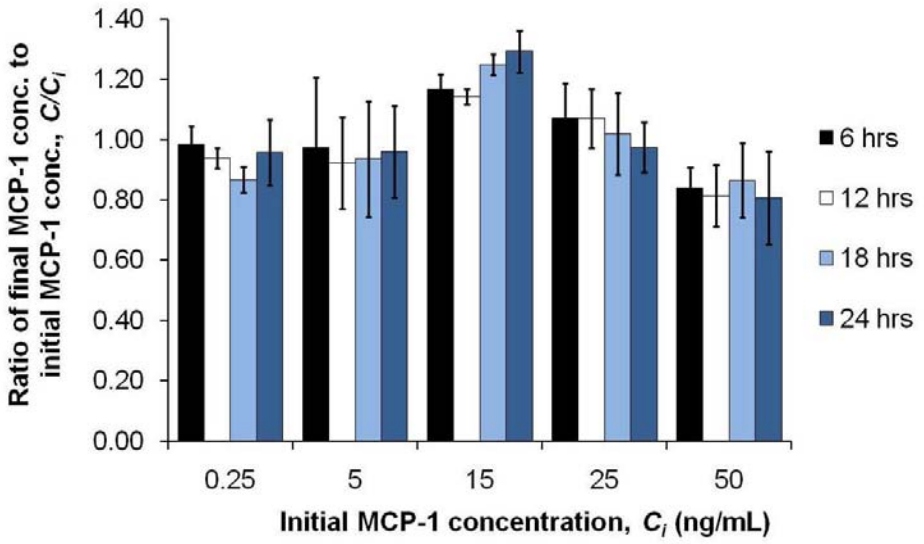

Figure 2.2 The stability of MCP-1 at standard conditions. Values are presented as mean ± SD. No significant change in concentration at later time points compared to the concentration at the 6-hour time point of samples within the same group (the same initial concentration) was observed.

MCP-1 binding reaction test

Another initial assumption was that MCP-1 does not bind with the collagen matrix. This assumption was tested using the 3D vascular tissue model without cells. Complete medium containing a set concentration of MCP-1 was added to the top reservoir of the 3D vascular tissue model. The following concentrations of MCP-1 were tested in the tissue model: 0.25, 5, 15, 25, or 50 ng/mL. The model was incubated at standard conditions to allow MCP-1 to diffuse from the top reservoir, through the collagen matrix, and into the bottom reservoir, which initially contained only complete medium. Samples taken from the top and the bottom reservoirs at different time points were analyzed for the concentration of MCP-1. The results are shown in **Figure 2.3**. MCP-1 concentrations in both the top and the bottom reservoirs of samples with initial top-reservoir concentration ($C_{i,top}$) of 0.25 ng/mL were lower than the detection range of the ELISA kit that we used. So, there is no data from those samples displayed in the figure.

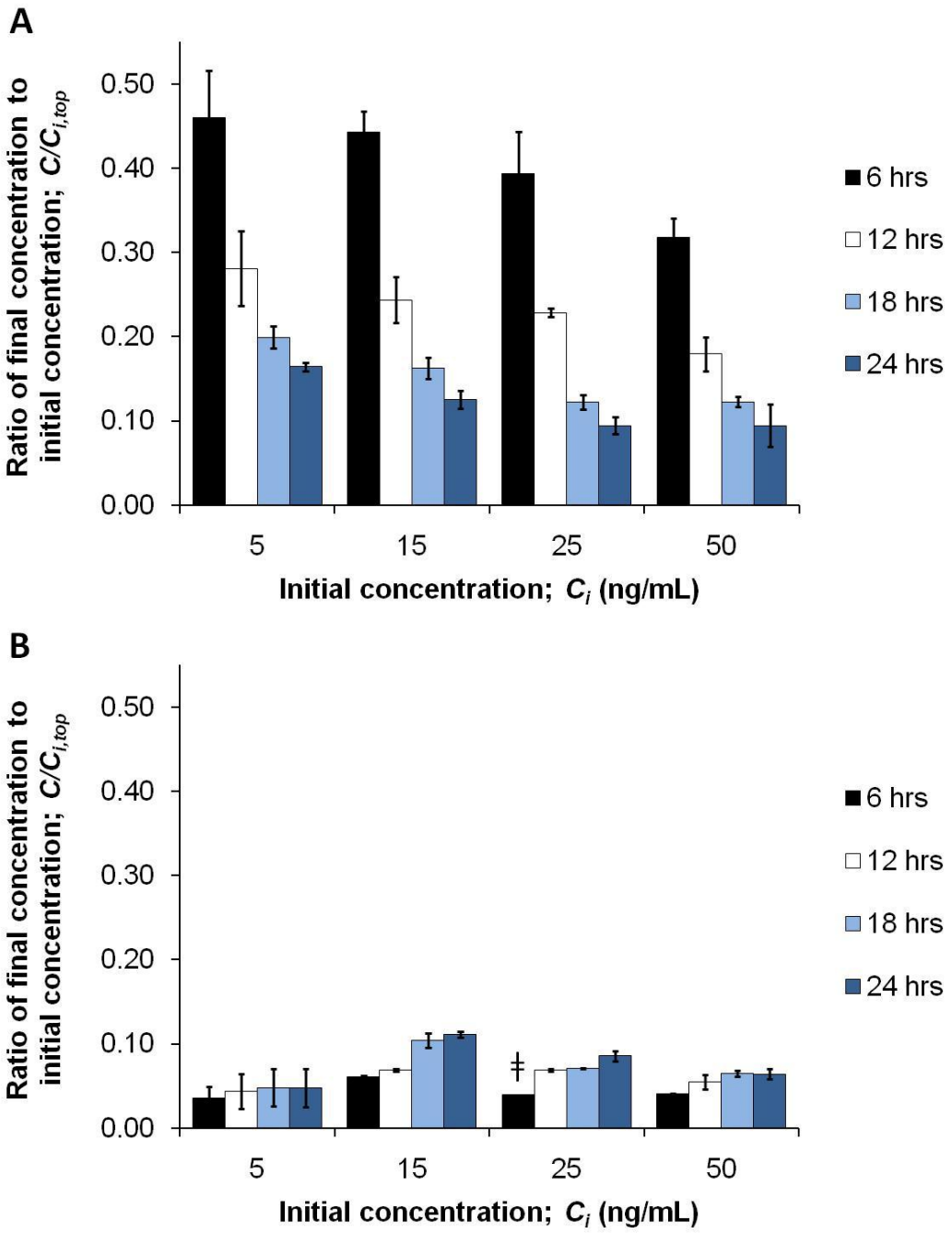

Figure 2.3 Concentration of MCP-1 in the top (*A*) and the bottom (*B*) reservoirs of the 3D vascular tissue model without cells. Values are presented as mean ± SD. ǂ represents the value of sample that is outside of the detection range. So, the true value is equal to or greater than the value shown.

If the volume of the collagen matrix is known, then the data in **Figure 2.3** can be used to calculate the average concentration of MCP-1 in the collagen matrix at each time point. The collagen volume was found to be 13 μL, estimated by using the cross-sectional area of the membrane insert and the thickness of the collagen matrix, which was measured microscopically to be 0.37 ± 0.06 mm. Additional assumptions that were used to calculate the concentration of MCP-1 in the collagen matrix include the following: (1) the volumes of the top and the bottom reservoirs, and the collagen matrix are constant, and (2) the contents in the top and the bottom reservoirs are well mixed. Results of the calculation showed that the average concentration of MCP-1 in the collagen matrix is higher than the concentration of MCP-1 in the top reservoir for all time points (**Table 2.1**).

However, for this experimental system, the concentration of MCP-1 in the collagen matrix cannot be higher than the concentration in the top reservoir, if there is no reaction inside the collagen matrix. The addition of MCP-1 to the top reservoir produces a concentration gradient, which drives the diffusion of MCP-1 through the collagen matrix and into the bottom reservoir. The diffusion will continue until MCP-1 concentration in the system is uniformed. Therefore, it is not possible that the concentration of MCP-1 in the collagen matrix is higher than in the top reservoir unless there is a reaction that occurs inside the collagen matrix, which consumes MCP-1 or transforms it from a soluble to a nonsoluble form. Hence, this conclusion suggests that our initial assumption about MCP-1 binding is not accurate and that MCP-1 does bind with some receptors in the collagen matrix.

Table 2.1 Average concentration of MCP-1 in the collagen matrix.

Samples	Ratio of MCP-1 concentration at current time point to initial MCP-1 concentration in top reservoir, *C/Ci,top*			
	6 hrs	12 hrs	18 hrs	24 hrs
$C_{i,top}$ = 5 ng/mL				
Top reservoir	0.460 ± 0.056	0.281 ± 0.044	0.199 ± 0.013	0.165 ± 0.005
Collagen matrix	2.36 ± 0.27**	3.34 ± 0.72**	3.77 ± 1.13**	4.06 ± 1.13**
$C_{i,top}$ = 15 ng/mL				
Top reservoir	0.443 ± 0.024	0.243 ± 0.027	0.163 ± 0.013	0.125 ± 0.010
Collagen matrix	1.25 ± 0.17*	2.39 ± 0.19**	1.24 ± 0.42*	1.17 ± 0.10**
$C_{i,top}$ = 25 ng/mL				
Top reservoir	0.394 ± 0.050	0.229 ± 0.005	0.123 ± 0.009	0.094 ± 0.010
Collagen matrix	≤ 2.66 ± 0.38	2.51 ± 0.09**	3.21 ± 0.06**	2.68 ± 0.21**
$C_{i,top}$ = 50 ng/mL				
Top reservoir	0.318 ± 0.023	0.179 ± 0.020	0.122 ± 0.006	0.094 ± 0.025
Collagen matrix	3.09 ± 0.08**	3.48 ± 0.53**	3.51 ± 0.15**	3.61 ± 0.28**

$C_{i,top}$ represents the initial MCP-1 concentration in the top reservoir. Values shown in the table are presented as mean ± SD, * $p < 0.05$ or ** $p < 0.01$ for change between MCP-1 concentration in the collagen matrix and the top reservoir at each time point.

Model development:

Governing equations

The experimental results showed that MCP-1 is stable at standard conditions for at least 24 hours and it binds with the collagen matrix. We assumed that the binding reaction between MCP-1 and the collagen matrix follows the general ligand-receptor reaction kinetics. Evidence from a study by Distler et al. [29] has shown that, if the binding reaction exists, it should be an irreversible reaction. Taking these experimental findings into consideration, the equation that represents the binding reaction between MCP-1 and the collagen matrix can be displayed as

$$M + S \rightarrow M \cdot S \tag{2.2}$$

where M is MCP-1, S is a binding site in the collagen matrix, and $M{\cdot}S$ is a MCP-1-binding-site complex. To derive the rate term of the mathematical model, it was assumed further that for the range of MCP-1 concentrations used in this study, the rate of consumption of MCP-1 due to the binding reaction follows the first-order kinetics. However, Michaelis-Menten kinetics or Langmuir isotherm should be applied to the rate term when higher concentration of MCP-1 is used [30].

$$R_M = -K_b C_M(z,t) \tag{2.3}$$

In equation (2.3), K_b is the rate constant for the binding reaction. By substituting equation (2.3) into equation (2.1), the model equation becomes

$$\frac{\partial C_M(z,t)}{\partial t} = D_{M|C}\left(\frac{\partial^2 C_M(z,t)}{\partial z^2}\right) - K_b C_M(z,t) \tag{2.4}$$

Equation (2.4) can also be referred to as the mass balance equation of MCP-1 in the collagen matrix. The concentration gradient of MCP-1 in the matrix can be determined by solving this equation.

After determining that MCP-1 can bind with the collagen matrix to form MCP-1-binding-site (*M·S*) complex, we would also like to determine the concentration profile of the *M·S* complex in the matrix, as it may have a haptotactic effect on monocyte migration. The equation of continuity was used again to develop the equation to represent the concentration of the *M·S* complex. However, unlike MCP-1, which can diffuse through the collagen matrix, the *M·S* complex is assumed to be fixed inside the matrix. Thus, the kinetics is the only concern in this case, and the equation to determine the concentration of the *M·S* complex was derived as

$$\frac{\partial C_{M\cdot S}(z,t)}{\partial t} = R_{M\cdot S}(z,t) \tag{2.5}$$

where $C_{M\cdot S}$ is the molar concentration of the *M·S* complex, and $R_{M\cdot S}$ is the rate of reaction of the *M·S* complex. We know from equation (2.2) that the rate of production of the *M·S* complex is equal to the negative value of the rate of consumption of MCP-1, or

$$R_{M\cdot S} = -R_M = K_b C_M(z,t) \tag{2.6}$$

Combining equations (2.5) and (2.6) , the equation to determine the concentration of the *M·S* complex, or the mass balance equation of the *M·S* complex in the collagen matrix, becomes

$$\frac{\partial C_{M\cdot S}(z,t)}{\partial t} = K_b C_M(z,t) \tag{2.7}$$

Boundary conditions

To solve equations (2.4) and (2.7), two initial conditions for C_M and $C_{M\cdot S}$ and two boundary conditions for C_M are required. All conditions were based on the assumptions that the top and bottom reservoirs are well mixed, and the concentrations of MCP-1 at the top and the bottom surface of the collagen matrix are equal to the concentrations in the top and the bottom reservoirs, respectively. Initial conditions were derived from the fact that initially, there was no MCP-1 in the collagen matrix or the bottom reservoir, and the concentration of MCP-1 in the top reservoir was known.

$$C_M(z,0) = 0 \tag{2.8}$$

$$C_M(0,0) = C_{i,top} \tag{2.9}$$

Because MCP-1 was added into the top reservoir, there was no binding reaction taking place at the beginning and the concentration of the $M\cdot S$ complex was equal to zero for all locations.

$$C_{M\cdot S}(z,0) = 0 \tag{2.10}$$

Next, the boundary conditions of C_M were derived from the mass balance equations of MCP-1 in the top and the bottom reservoirs when $t > 0$. Since the concentration of MCP-1 in the top reservoir is assumed to be equal to the concentration at the top surface of the collagen matrix, the convective mass transfer of MCP-1 from the bulk of the top reservoir to the collagen surface is neglected. Thus, the rate of change of MCP-1 concentration in the top reservoir depends only on the rate of MCP-1 that diffuses through the top surface of the collagen matrix.

$$\frac{\partial C_M(0,t)}{\partial t} = \left(\frac{D_{M|C} A_{top\ surface}}{V_{top\ reservoir}}\right)\left(\frac{\partial C_M(0,t)}{\partial z}\right) \quad (2.11)$$

The relationship is the same for the change of MCP-1 concentration in the bottom reservoir and the diffusion of MCP-1 through the bottom surface of the collagen matrix. A negative sign was added to the following equation, to show the direction of MCP-1 diffusing from the collagen matrix to the bottom reservoir.

$$\frac{\partial C_M(z_f,t)}{\partial t} = -\left(\frac{D_{M|C} A_{bottom\ surface}}{V_{bottom\ reservoir}}\right)\left(\frac{\partial C_M(z_f,t)}{\partial z}\right) \quad (2.12)$$

In equations (2.11) and (2.12), A is the surface area of either the top or the bottom surface of the collagen matrix, V is the volume of the top or the bottom reservoir, and z_f is the thickness of the collagen matrix. The area of the top and the bottom surface of the collagen matrix is assumed to be equal to the cross-sectional area of the membrane insert of the Transwell® plate. The volumes of the top and the bottom reservoirs are the values set for the experiments.

Numerical solution:

There were two unknown constants, $D_{M|C}$ and K_b, in the mathematical model. Their values were estimated by fitting the results of the mathematical model to experimental data. Data from **Figure 2.3**, when the initial concentration of MCP-1 in the top reservoir was 5, 15, or 50 ng/mL, were selected for the regression. The mathematical model was solved in MS-Excel with VBA using the Crank-Nicolson numerical method. The values of $D_{M|C}$ and K_b were determined by fitting the calculated results to the selected experimental data, using the weighted least squares method.

To validate the estimated values of $D_{M|C}$ and K_b, and to evaluate the mathematical model, the initial concentration of MCP-1 in the top reservoir of 25 ng/mL was used to compare the model results to the experimental results.

Numerical results:

Parameter estimation

We found that the values of $D_{M|C}$ and K_b that gave the best fit to the selected experimental data are 0.108 mm^2/hr and 0.858 hr^{-1}, respectively. Results of the regression are displayed in **Figure 2.4**. From the figure, the data calculated from the mathematical model are about the average of the experimental data with the overall %AAD of 18.0%. When considering the correlation results of the MCP-1 concentration in the top and the bottom reservoirs separately, the %AADs for the top- and bottom-reservoir concentrations are 21.0% and 15.1%, respectively.

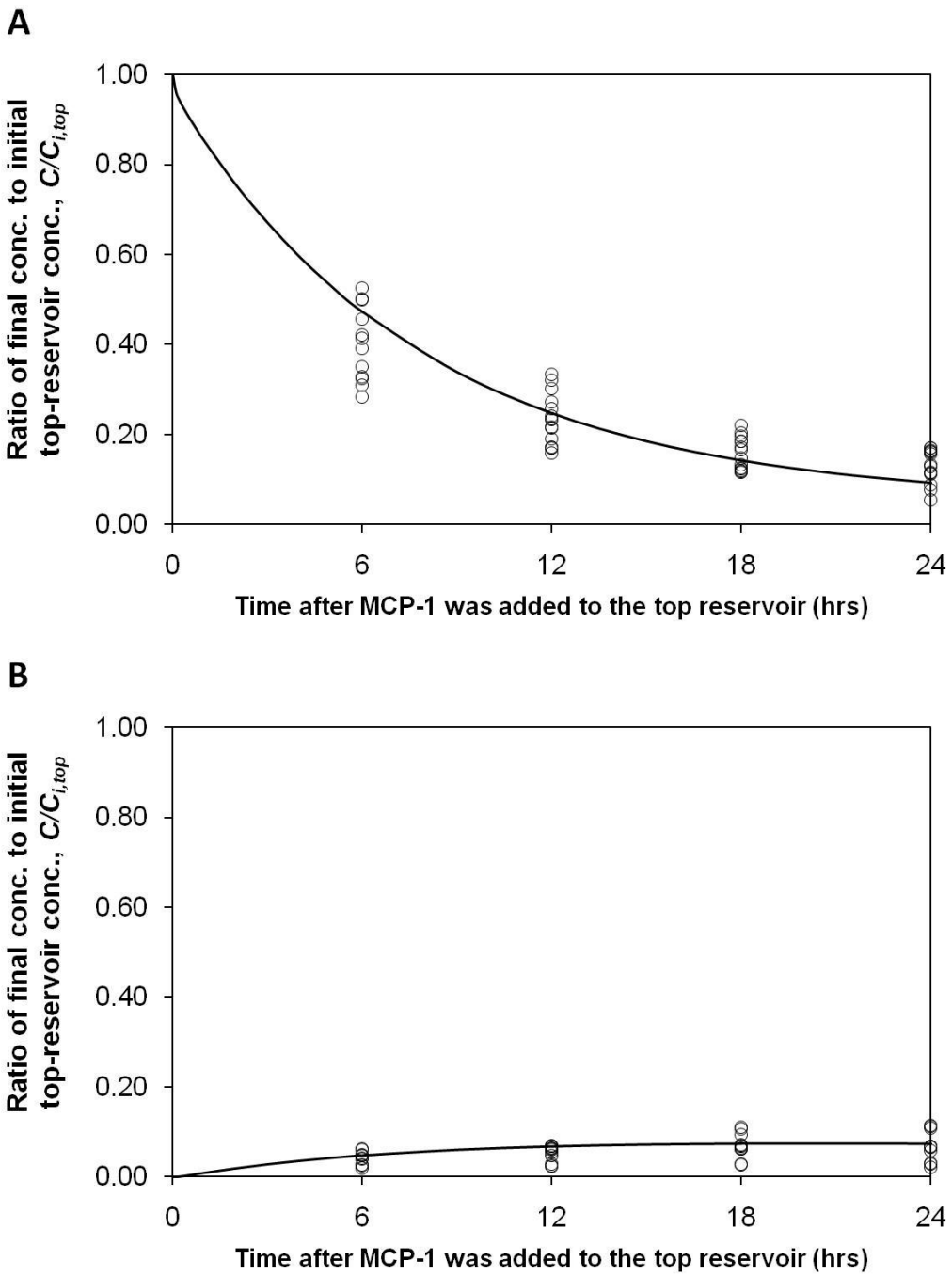

Figure 2.4 Experimental and correlated concentrations of MCP-1 in the top (*A*) and the bottom (*B*) reservoirs when initial MCP-1 concentration in the top reservoir was 5, 15, or 50 ng/mL. Experimental data are displayed as circle markers, while data from the mathematical model are displayed as a solid line.

Validation of the mathematical model

The mathematical model, together with the estimated values of $D_{M|C}$ and K_b, were validated with the experimental data shown in **Figure 2.3**, when the initial concentration of MCP-1 in the top reservoir was 25 ng/mL. The validation results are displayed in **Figure 2.5**. As observed from the figure, the mathematical model demonstrated a good prediction of MCP-1 concentrations in both the top and the bottom reservoirs. The overall %AAD between the predicted and experimental results is 10.8%, with %AADs equal to 13.7% for the top-reservoir calculation and 6.8% for the bottom-reservoir calculation. This low value of deviation shows that the transportation of MCP-1 in the 3D tissue model in the first 24 hours can be represented by the formulated mathematical model for the initial concentration of MCP-1 in the top reservoir between 5 and 50 ng/mL. It is important to note here that we did not know the actual MCP-1 concentration in the bottom reservoir at time equal to six hours. Due to the dilution factor used for sample dilution during ELISA, the detected concentration of this group of samples is greater than the detection range of the ELISA kit. Therefore, the experimental data at that time point was not used in the mathematical-model validation, and is not displayed in **Figure 2.5**.

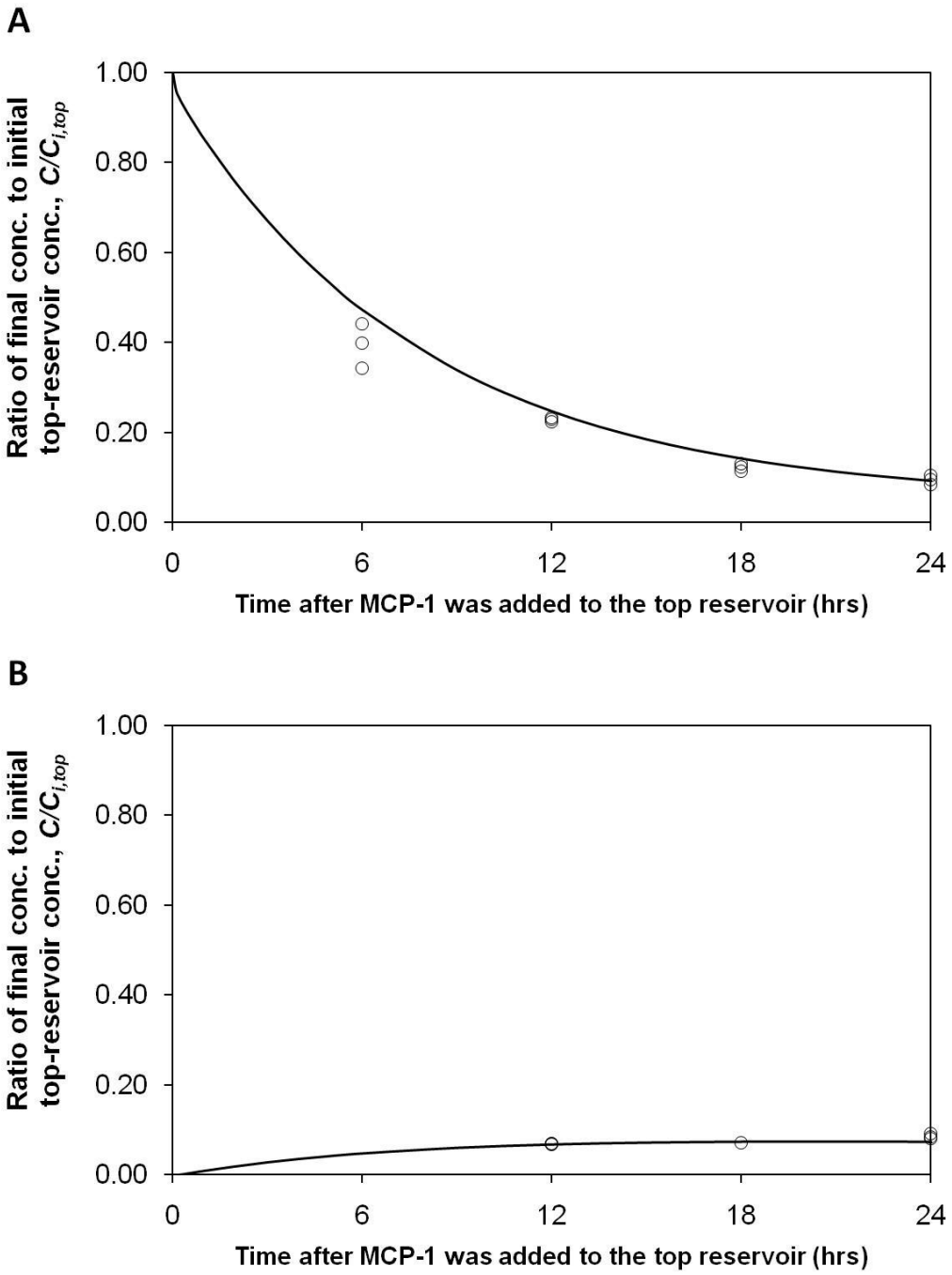

Figure 2.5 Predicted and experimental concentrations in the top (*A*) and the bottom (*B*) reservoirs when initial MCP-1 concentration in the top reservoir was 25 ng/mL. Experimental data are displayed as circle markers, while data from the model are displayed as a solid line.

MCP-1 concentration gradient in the collagen matrix

The concentration gradients of MCP-1, both soluble and static (bound), were calculated using the mathematical model. Plots showing the concentration of MCP-1 as a function of distance from the top surface of the collagen matrix are presented in **Figure 2.6**. The concentration gradient of soluble MCP-1 appears to be linearly dependent on the distance at any time point, and such gradient diminishes over time. Contrarily, the concentration gradient of MCP-1 that binds to the binding sites, or the static gradient of MCP-1, increases as time passed and overcomes the soluble gradient of MCP-1 after two hours (data are not shown in the figure). This finding suggests that, apart from the soluble gradient of MCP-1, the static gradient of MCP-1 is another potent factor that may mediate monocyte transendothelial migration.

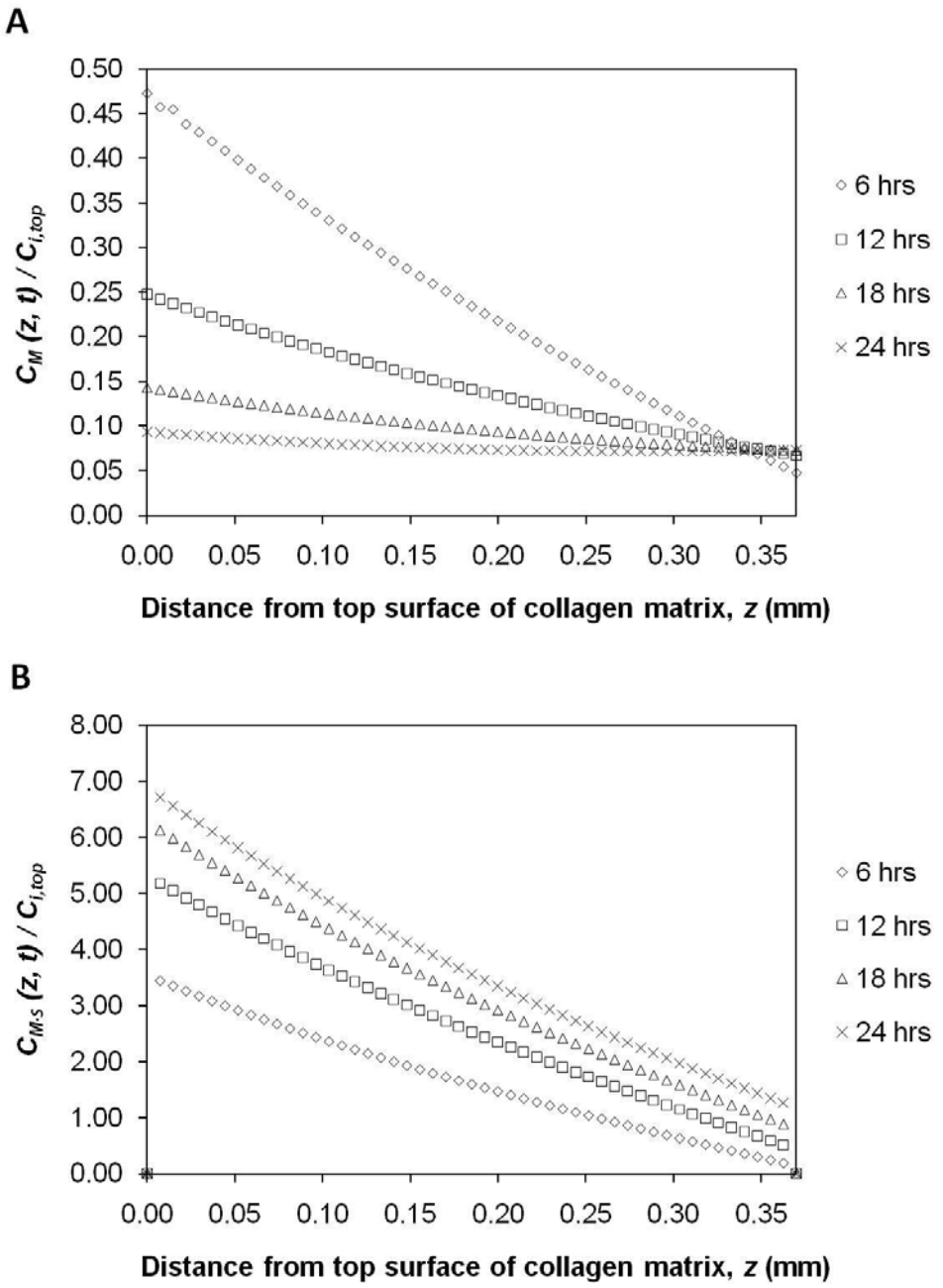

Figure 2.6 Concentration gradients of MCP-1 in the collagen matrix. **Figure 2.6*A*** shows the ratio of the concentration of MCP-1 that is soluble in the collagen matrix (C_M *(z, t)*) to the initial concentration of MCP-1 in the top reservoir ($C_{i,top}$). **Figure 2.6*B*** shows the ratio of the concentration of MCP-1 that binds with the collagen matrix ($C_{M\cdot S}$ *(z, t)*) to the initial concentration of MCP-1 in the top reservoir.

Discussion:

In the present study, we developed a mathematical model to determine the concentration gradient of MCP-1 that formed in the collagen matrix of the 3D *in vitro* vascular tissue model without cells. Both kinetic and transport behaviors were taken into account for the mathematical model development. For the kinetics, the mathematical model focused mainly on the stability of MCP-1 at standard conditions and the reaction between MCP-1 and the collagen matrix. Our experimental results demonstrate that MCP-1 is stable for at least 24 hours when it is presented as a solute in complete medium. However, this finding applies for recombinant MCP-1 only. When endothelial cells are added to the tissue model, the stability of MCP-1 will be reevaluated, because other substances produced by the cells may affect MCP-1 stability.

A binding reaction between MCP-1 and the collagen matrix is another aspect that we considered during the development of the mathematical model. Experiments were conducted with the 3D tissue model to determine whether the binding reaction existed. We concluded from experimental results that MCP-1 does bind with the collagen matrix. Another study investigated the time-dependent release of MCP-1 from Type 1 collagen, which is the main component in the collagen solution used for this study. Results from this study showed that no release of MCP-1 was detected in the first 72 hours [29]. This result agrees with the assumption that the binding reaction between MCP-1 and the collagen matrix can be considered as an irreversible reaction.

Based on the knowledge about the MCP-1 binding reaction, two equations that represent the mass balance of MCP-1 and the $M{\cdot}S$ complex in the collagen matrix were

developed. The values of two unknown constants, $D_{M|C}$ and K_b, which appear in the mathematical model, were found to be 0.108 mm^2/hr and 0.858 hr^{-1}, respectively. The value of $D_{M|C}$ in this study is lower than the one calculated from an empirical equation used in the study of Zhao et al. [31] (0.247 mm^2/hr) or the one reported in the study of Fleury et al. [32] for bioactive molecules that are in the same family as MCP-1 and have molecular weights close to MCP-1 (0.468-0.576 mm^2/hr). The difference in the values could be due to the methods used to determine the values. In this study, the parameter $D_{M|C}$ was determined based on experimental data, while empirical equations for the estimation of the diffusivity coefficient in water and correction factors were used to estimate $D_{M|C}$ in the other two studies.

Results of the mathematical model show that the concentration gradient of soluble MCP-1 decreases over time; whereas, the static gradient of MCP-1 increases. This finding is reasonable and expected for a system with a single administration of MCP-1 and with the irreversible binding reaction. Interestingly, the concentration of static MCP-1, or the MCP-1 that binds with the collagen matrix, is higher than that of the soluble MCP-1 after two hours. This observation is opposite to the results of a previous study, which showed that when applied to amnion membrane, most of the MCP-1 appears in a soluble form [13]. This could be due to the fact that the amnion membrane is very thin, by an order of magnitude, when compared to the collagen matrix used in this study. Moreover, the Type 1 collagen content in the amnion membrane is not as high as in the collagen matrix. Both differences could result in fewer possible binding sites for MCP-1 in the amnion membrane compared to the collagen matrix used in this study.

In conclusion, a mathematical model to determine the concentration gradients of MCP-1 in a collagen matrix of a 3D vascular tissue model without cells was developed in this study. Results of our experiments and the mathematical model suggest that there should be a binding reaction of MCP-1 with the collagen matrix, and such a reaction can produce a static gradient of MCP-1 across the matrix. We hypothesize that the static gradient may also play a role during the transendothelial migration of monocytes, and recommend that more investigations should be done to ensure the existence of the binding reaction. Furthermore, we expect that the use of this mathematical model, together with the 3D vascular tissue model, will provide a way to study the formation of the gradient of MCP-1 that is secreted from endothelial cells and the effect of the gradient on monocyte migration involved in the early stages of atherosclerosis.

CHAPTER III

EFFECT OF STORAGE CONDITIONS ON THE STABILITY OF RECOMBINANT HUMAN MCP-1/CCL2

Chemokines (chemotatic cytokines) are low molecular weight proteins (8-12 kDa) that play an important role in the migration of immune cells [33]. Their functions involve with homeostatic mechanisms, e.g., lymphocyte trafficking or immune surveillance, as well as inflammatory activities, such as recruiting lymphocytes to an injured area [34, 35]. Monocyte chemoattractant protein-1 (MCP-1 or CCL2) is a chemokine that is secreted by various cell types and involves in the progression of many inflammatory-related diseases including HIV, cancer, and atherosclerosis [36]. The key function of MCP-1 during inflammation is to mediate the recruitment, migration, and infiltration of monocytes to an infected site [37].

Since MCP-1 was first purified more than two decades ago [38-40], a number of studies have been done to characterize and relate it to the pathogenesis of many diseases [36, 37, 41]. With the advancements in technology, MCP-1 is now commercially available for laboratory use in the form of recombinant protein. Recombinant MCP-1 is frequently used in many *in vitro* studies [42-45] including those that focus on the transendothelial migration of monocytes [15, 46]. In our previous study, we used

recombinant human MCP-1 to examine the formation of MCP-1 concentration gradients across the collagen matrix of a 3D *in vitro* vascular tissue model (Manuscript in review). Briefly, recombinant MCP-1 was added to the system, samples were collected from the system at various time points, and the concentration of MCP-1 in the samples were determined by ELISA. The gradients of MCP-1 in the collagen matrix were estimated based on the concentration data. To achieve an accurate estimation of the amount of MCP-1 in the system, it is important to measure accurately the concentration of MCP-1 in the samples collected from the system. Since the collected samples are stored at -81°C until ready for analysis, this raises a concern about the loss of MCP-1 during storage.

Generally, it is suggested that recombinant MCP-1 should be stored at high concentration (10 μg/mL or greater) to maintain the stability of the protein. During an experiment, recombinant MCP-1 is diluted to physiological relevant concentrations, with working concentrations in the pg/mL to ng/mL range [15, 42-46]. Consequently, samples that are collected from such experimental systems contain recombinant MCP-1 at lower concentrations than the suggested value for storage. Thus, if those samples are not analyzed immediately, some MCP-1 molecules in the samples may become unstable over time.

In the present study, we investigated the effect of storing conditions on the loss of MCP-1 in samples containing recombinant human MCP-1 at the working concentrations. The objectives of this study include determining 1) the loss of MCP-1 at different storage conditions and 2) the effect of multiple freeze-thaw cycles to the stability of MCP-1 in the samples. Results of this study were aimed to provide a guideline to handle samples

that contain recombinant human MCP-1, but can also be applied to other recombinant proteins used at low working concentrations.

Materials and methods:

Materials

Recombinant human MCP-1 was purchased from R&D Systems (Minneapolis, MN). Dulbecco's phosphate-buffered saline (D-PBS), Medium 199, and penicillin-streptomycin-glutamine (PSG) solution were purchased from Invitrogen (Carlsbard, CA). Fetal bovine serum (FBS) was purchased from Hyclone (Logan, UT). Tween® 20 was purchased from Fisher Scientific (Pittsburgh, PA). Bovine serum albumin (BSA) was purchased from Sigma-Aldrich (St. Louis, MO). BD OptEIA™ Human MCP-1 ELISA Set was purchased from BD Biosciences (San Jose, CA).

Experiments

MCP-1 solutions were prepared from recombinant human MCP-1 and complete medium (Medium M199 containing 1% PSG and 10% FBS) at the following concentrations: 0.25, 5, 15, 25, and 50 ng/mL. The prepared solutions were stored at standard conditions (37°C and humidified atmosphere of 5% CO_2 and 95% air), 4°C, -20°C, or -81°C for seven days. On the seventh day, samples were collected from the solutions and analyzed immediately for the concentration of MCP-1. After collecting the samples, the solutions that were previously stored at freezing conditions (-20°C and -81°C) were frozen again at the same conditions for one more day before being thawed and analyzed again to determine the effect of multiple freeze-thaw cycles.

ELISA

MCP-1 ELISA was performed as instructed in the manufacturer's manual, except that complete medium was used as diluents for standards and samples instead of Assay Diluent. The plates were assayed on an Emax precision microplate reader (Molecular Devices, Sunnyvale, CA) at the 450 nm wavelength subtracted by the 540 nm reference wavelength. MCP-1 concentrations were determined by comparing absorbance readings to a standard curve developed from the same assay.

Statistical analysis

MCP-1 concentrations are expressed as mean ± SD of three samples. Significant differences in the results were determined using student's *t* test. A value of $p < 0.05$ was considered significant.

Results:

Storing conditions

To determine the effect of storage conditions to the loss of MCP-1 in samples, MCP-1 solutions were prepared from recombinant human MCP-1 and complete medium, and stored at different conditions for seven days. ELISA was performed at the end of the storage time to determine the concentration of MCP-1. Results are represented in **Figure 3.1**. As shown in the figure, there is no significant change in the concentration of MCP-1 among samples with the same initial concentration, except for the 50 ng/mL samples in which the significant loss of MCP-1 is observed in samples that were stored at freezing conditions. Results also show that if the data from 50 ng/mL samples are excluded, the

percent recovery of MCP-1 varies between 80% and 100%. These two findings suggest that for samples with low MCP-1 concentration (≤ 25 ng/mL), recombinant human MCP-1 in the samples is stable for all of the storage conditions tested for the seven days. Moreover, when comparing results from samples that were stored at non-freezing conditions to those stored at freezing conditions, it appears that the first freeze-thaw cycle does not affect the MCP-1 stability in the samples, as shown by no significant change in the concentration of the samples. However, the same conclusion does not apply to 50 ng/mL samples. Because the significant loss of MCP-1 is only found in 50 ng/mL samples that were stored at freezing conditions, we believe that the loss is due to the freeze-thaw process and is concentration dependent.

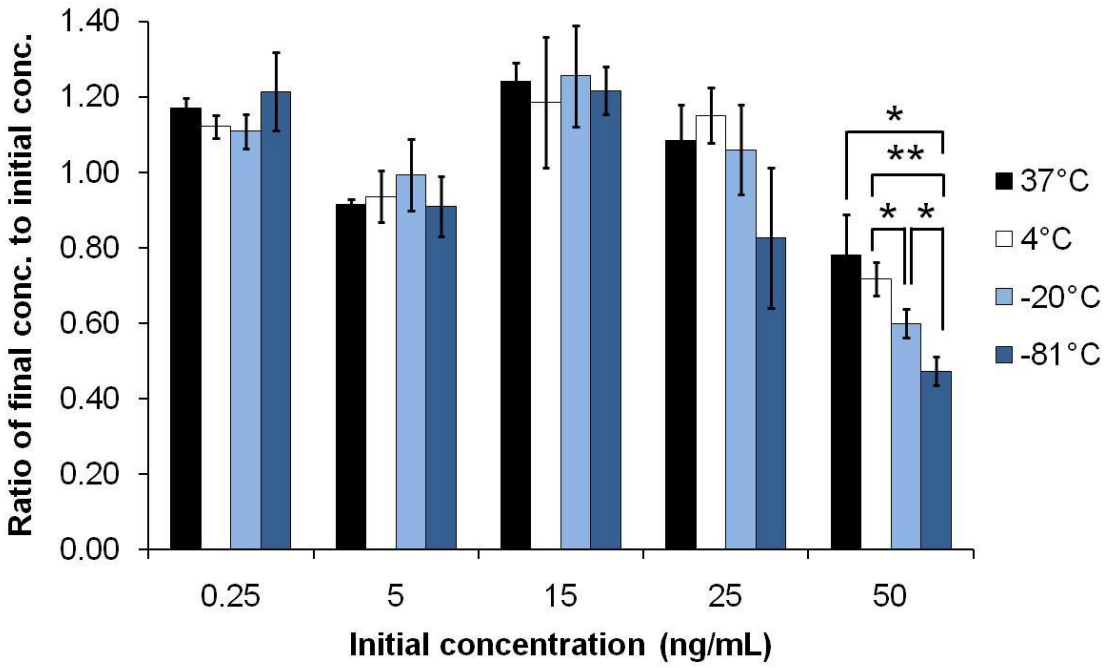

Figure 3.1 The effect of storage conditions to the stability of MCP-1. Values are presented as mean ± SD, * $p < 0.05$ and ** $p < 0.01$ for changes in the concentration.

Multiple freeze-thaw cycles

The test to determine the effect of multiple freeze-thaw cycles was carried out after the end of the seven-day storage. MCP-1 solutions that were previously stored at -20°C or -81°C were collected and frozen again at the same conditions for 24 hours. The samples were thawed for the second time and analyzed for the concentration of MCP-1. The concentration was found to decrease significantly after the second thaw for most of the samples that were stored at -20°C and -81°C (**Figure 3.2**). The average percentage loss of MCP-1 due to the second thaw is 48% and 49% for the samples stored at -20°C and -81°C, respectively. These results demonstrate that unlike the first freeze-thaw cycle, which affects only samples with high concentrations, the second freeze-thaw cycles results in approximately a 50% loss to recombinant human MCP-1 in all samples, regardless of the freezing conditions.

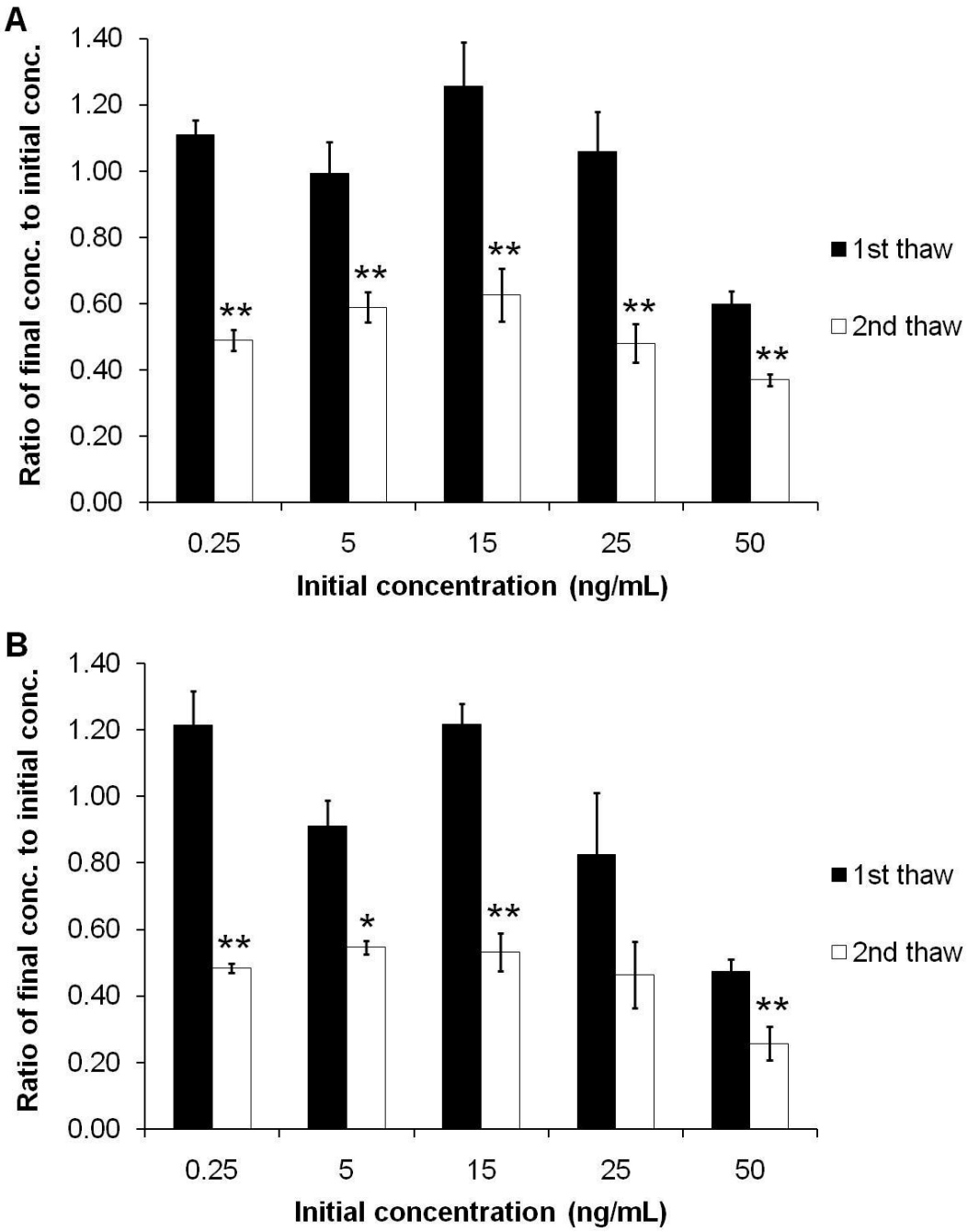

Figure 3.2 The effect of freeze-thaw cycle(s) to the stability of MCP-1. Freezing conditions were selected to be -20°C (*A*) or -81°C (*B*). Values are represented as mean ± SD, * $p < 0.05$ and ** $p < 0.01$ for changes in MCP-1 concentration after the second thaw, compared to results from the first thaw.

Discussion:

The use of recombinant MCP-1 in an *in vitro* study generally requires that the recombinant protein is diluted from the stock concentration in the µg/mL range to the working concentrations in the pg/mL to ng/mL range. For many studies, samples containing MCP-1 at the working concentrations are stored and analyzed at the end of an experiment to determine the concentration of MCP-1. The stability of recombinant MCP-1 in samples may not be an issue if the analysis can be performed immediately after the collection of the samples. However, it may be unavoidable that the samples must be stored for a period of time before being analyzed. In this case, MCP-1 stability needs to be confirmed in order to ensure that the analyzed concentration of MCP-1 represents the actual concentration in the samples at the time they were collected.

In the present study, the stability of recombinant human MCP-1 during storage was examined. MCP-1 solutions were stored at different conditions for seven days to evaluate the effect of short term storage. Results show that for most of the solutions, recombinant MCP-1 is stable for at least seven days for all conditions tested. It can also be deduced from the same results that the first freeze-thaw cycle does not affect the concentration of MCP-1 in most of the solutions. However, the stability of recombinant MCP-1 seems to decrease as the concentration of MCP-1 in the solutions increases. Because the significant loss of MCP-1 was only observed in the solution that was stored at freezing conditions and contained the high level of MCP-1 (50 ng/mL), we believe that the first freeze-thaw cycle is a major contributor to such a loss and that the loss is concentration dependent.

In our previous study, we demonstrated that recombinant human MCP-1 is stable at standard conditions for at least 24 hours (Manuscript in review). Samples were collected every six hours from MCP-1 solutions that were incubated at standard conditions and stored at -81°C for one to four days before being analyzed for the concentration of MCP-1. As shown in **Figure 3.3** there is no significant difference between the concentration of samples stored at 37°C for seven days (from the current study) and that of samples stored at standard conditions for 6-24 hours (from the previous study). This finding agrees with our conclusion that recombinant human MCP-1 is stable for at least seven days. Interestingly, it appears in the figure that the freeze-thaw cycle did not affect the stability of MCP-1 in the previous study as it did in the present study for the 50 ng/mL samples. Since in the previous study, samples were stored at -81°C for no more than four days, we question that time may be another factor that affects the loss of MCP-1 during the first freeze-thaw cycle.

The effect of multiple freeze-thaw cycles is another aspect being investigated in the present study. Experimental results show that for both freezing conditions (-20°C and -81°C), the second freeze-thaw cycle causes nearly a 50% loss to the concentration of MCP-1 in samples. This demonstrates that repeatedly freezing and thawing samples should be avoided. Since the loss to the samples is constant, the concentration of samples that have gone through two freeze-thaw cycles can still be estimated. The actual concentration of MCP-1 in the samples is approximately two times the concentration measured from an analysis after the second thaw.

Briefly, the stability of recombinant human MCP-1 when it is stored at working concentrations was investigated in this study. Experimental results show that samples

containing recombinant human MCP-1 can be stored at non-freezing condition for a short term without significant loss of MCP-1. However, we recommend that if samples are stored at freezing conditions, they should be analyzed as soon as possible because evidence shows that the loss of MCP-1 during the first freeze-thaw cycle may be time dependent. Also, in the case of storing the samples frozen, multiple freeze-thaw cycles can lead to a significant loss of MCP-1 in samples and should be avoided.

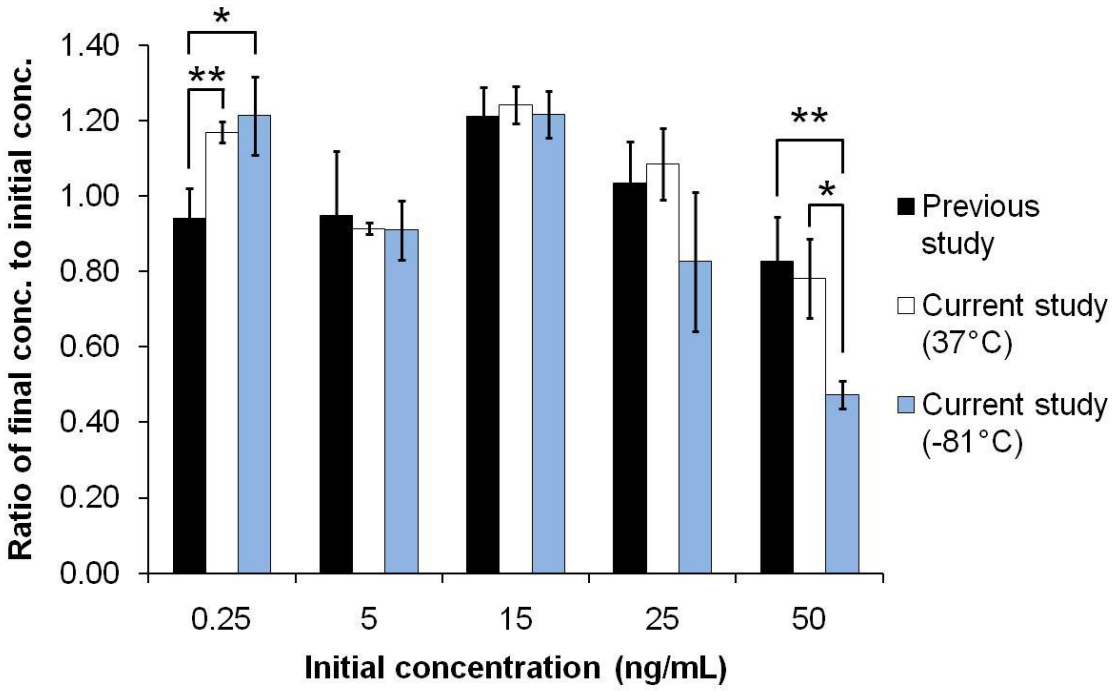

Figure 3.3 The comparison between results from previous and current studies. Data labeled as "Previous study" are the average concentration of MCP-1 solutions that were incubated at standard conditions for 6-24 hours, and subsequently stored at -81°C for one to four days. The concentration of MCP-1 solutions after stored at either standard conditions or -81°C for seven days is obtained from data in **Figure 3.1** and presented as "Current study (37°C)" or "Current study (-81°C)". Values are represented as mean ± SD, * $p < 0.05$ and ** $p < 0.01$ for difference in MCP-1 concentration.

CHAPTER IV

THE FORMATION OF A STATIC CONCENTRATION GRADIENT OF MCP-1 IN A COLLAGEN MATRIX AND ITS HAPTOTACTIC EFFECT ON MONOCYTE MIGRATION

Atherosclerosis is an inflammatory disease [6] in which its initiation involves the infiltration of leukocytes into the vascular intima [5, 7]. An injury to the endothelium of a blood vessel and subsequent endothelial dysfunction are believed to be the cause of atherosclerosis formation [6]. Factors that may induce the injury include hypercholesterolemia, hypertension, diabetes, and smoking [5, 6]. The process in which leukocytes in the bloodstream are recruited into the injured area includes the tethering and slow rolling of blood-borne leukocytes on activated endothelial cells, the adhesion of leukocytes to the endothelium, and finally, the intravascular crawling and transmigration of leukocytes across the endothelial layer [10]. Each of these steps is activated by cellular adhesion molecules and cytokines.

Monocyte chemoattractant protein-1 (MCP-1 or CCL2) is a chemokine in the CC family that is believed to play an important role in mediating monocyte trafficking across the endothelial layer. MCP-1 is secreted by various cell types, including endothelial cells, smooth muscle cells, and monocytes (or macrophages), which

are commonly found in atherosclerosis plaque [47, 48]. The fact that MCP-1 is highly expressed in atherosclerosis lesions elicits interest concerning the involvement of MCP-1 in the development of this disease [23, 24, 49]. MCP-1 was confirmed to be crucial during the early stage of atherosclerosis by results from studies in murine models showing that the absence of MCP-1 reduces the formation of atherosclerosis lesion [25, 26]. Many *in vitro* studies demonstrate that one of the initial steps of atherosclerosis involving monocyte migration is directed by the soluble gradient of MCP-1 (chemotaxis) [13, 14, 50-52].

Although it is generally accepted that the direction of monocyte migration is in response to the soluble gradient of MCP-1, information about the formation of such a gradient across the endothelium is still limited. It was reported that MCP-1 is secreted from endothelial cells in a soluble form [27], and when the cells are stimulated, the secretion is found to be non-polarized, which means MCP-1 is secreted equally from the apical and basal sides of the cells [13]. Based on these two findings, Webber et al. suggested that *in vivo*, MCP-1 secreted from the apical side of the endothelium is continuously removed by blood flow in the lumen, while MCP-1 secreted from the basal side is maintained in the extracellular matrix (ECM) beneath the endothelium, thus forming a MCP-1 soluble gradient across the endothelium [27]. Previously, we examined the formation of a MCP-1 concentration gradient in the ECM using a simplified 3D *in vitro* vascular tissue model (without the addition of endothelial cells) and a mathematical model (Manuscript in review). Experimental results indicated that MCP-1 binds with collagen in the collagen matrix of the tissue model. We proposed that in this binding reaction, the soluble MCP-1 reacts with a binding site on the collagen, and a static MCP-

1-binding site complex is formed as a product. As a result, the static MCP-1 concentration gradient is created in the collagen matrix, along with the gradient of soluble MCP-1. Evidence from another study also suggested that the binding reaction may be irreversible [29].

In the current study, we tested the hypothesis that the static concentration gradient of MCP-1 presents a haptotactic effect on the migration of monocytes. The objectives of this paper are to verify the existence of the binding reaction between MCP-1 and collagen, and to examine the migration of moncytes in response to the static concentration gradient of MCP-1 (haptotaxis). The results of this study will provide a better understanding of the formation of MCP-1 concentration gradients in the ECM that are relevant to atherosclerosis.

Materials and methods:

Materials

Recombinant human MCP-1 was purchased from R&D Systems (Minneapolis, MN). Dulbecco's phosphate-buffered saline (D-PBS), Medium 199, penicillin-streptomycin-glutamine (PSG) solution, and Dynabeads® Untouched™ Human Monocytes kit were purchased from Invitrogen (Carlsbard, CA). Fetal bovine serum (FBS) was purchased from Hyclone (Logan, UT). PureCol® collagen (97% Type 1 collagen) was purchased from Advanced BioMatrix (San Diego, CA). Sodium hydroxide was purchased from VWR (West Chester, PA). Corning Transwell® permeable supports, 4% paraformaldehyde in PBS, and Tween® 20 were purchased from Fisher Scientific (Pittsburgh, PA). Ficoll-Paque™ PLUS was purchased from GE Healthcare

(Uppsala, Sweden). Bovine serum albumin (BSA) was purchased from Sigma-Aldrich (St. Louis, MO). BD OptEIA™ Human MCP-1 ELISA Set was purchased from BD Biosciences (San Jose, CA).

Preparation of the collage matrix of the 3D in vitro vascular tissue model

The collagen matrix of the 3D tissue model was prepared using a procedure similar to what described in our previous study [28]. (The schematic diagram of the 3D tissue model is shown in **Figure 4.1*A***). Briefly, collagen solution consisting of 57.1 vol% PureCol® collagen (3 mg/mL), 7.14 vol% Medium 199, and 35.7 vol% 0.1 M sodium hydroxide was added to a membrane insert of a Transwell® plate. The plate was incubated at standard conditions (37°C, and humidified atmosphere of 5% CO_2 and 95% air) for one hour to allow the collagen solution to gel. Complete medium containing 10 vol% FBS and 1 vol% PSG in Medium 199 was added to the top and bottom reservoirs of the tissue model. The plate was incubated at standard conditions for an additional 12 hours to equilibrate the collagen matrix. After aspirating complete medium from the tissue model, the collagen matrix was ready for testing.

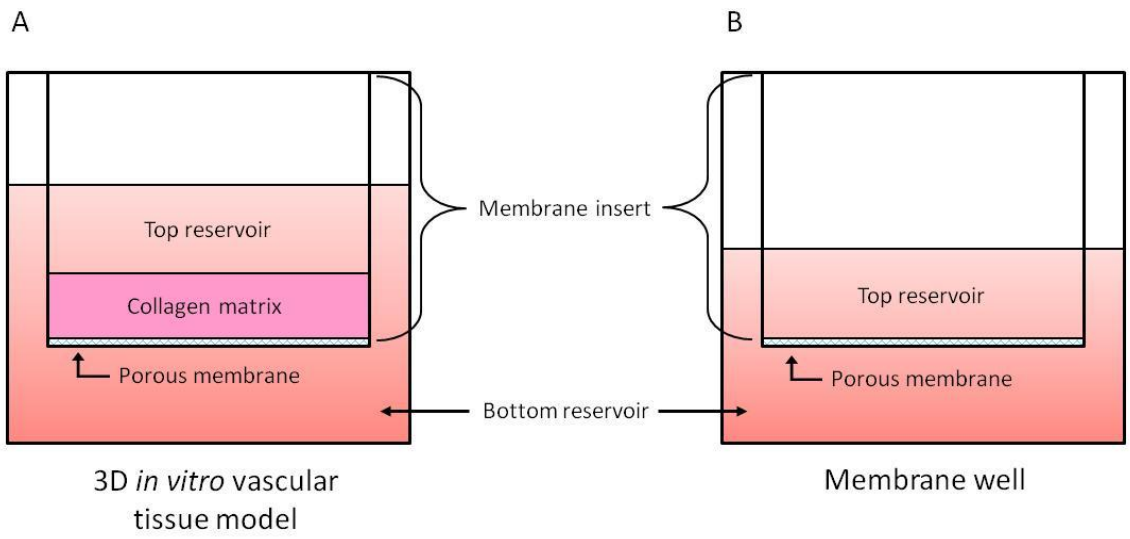

Figure 4.1 The schematic diagram of (*A*) 3D tissue model and (*B*) membrane well

Pre-treating collagen matrix with MCP-1

MCP-1 solution (50 ng/mL of MCP-1 in complete medium) was added into the top reservoir of the 3D tissue model with the collagen matrix, while the bottom reservoir of the model was filled with complete medium alone. MCP-1 was allowed to diffuse through and react with the collagen matrix by incubating the plate at standard conditions for 24 hours. Immediately after the incubation, samples were collected from the top and bottom reservoirs of the tissue model and both reservoirs were rinsed three times using complete medium to remove MCP-1 that may attach to the wall of the reservoirs. After that, three successive washes were performed to ensure that soluble MCP-1 in the collagen matrix is completely removed. Each successive wash was done by adding complete medium to the top and bottom reservoirs, placing the tissue model inside the incubator for one hour, and removing the remaining media from the top and bottom reservoirs. The removed media and the samples that were previously collected were

stored at -81°C until ready for an analysis. The concentration of MCP-1 in the samples was measured by ELISA.

Monocyte isolation method

Human peripheral blood mononuclear cells (PBMCs) were isolated by density gradient centrifugation on Ficoll-Paque PLUS™ from the blood obtained from healthy donors from the Oklahoma Blood Institute (OBI) (Oklahoma City, OK). Monocytes were separated from the PBMCs by magnetic bead separation. Dynabeads® Untouched™ Human Monocytes kit was used to negatively select monocytes from the PBMC population, using the standard protocol. Briefly, PBMCs were incubated at appropriate dilutions with magnetic beads coated with antibodies specific of all cell types within the PBMC population except for the monocyte population. The tube containing the labeled sample was placed into a tube holder that induces a high-gradient magnetic field on the tube wall. The labeled cells adhered to the inside surface of the tube wall, and the unlabeled monocytes were collected within the supernatant. The tube was rinsed several times to remove all the unlabeled monocytes. Monocytes were isolated from fresh blood samples and used directly in all experiments.

Migration assay

The collagen matrix of the 3D tissue model was prepared and either pre-treated with 50-ng/mL MCP-1 solutions as described in the section above, or used directly without pre-treating. Complete medium containing monocytes at the density of 750,000 cells/mL (2.27×10^5 cells/cm^2) was added to the top reservoir of the 3D tissue model, and complete medium alone was added to the bottom reservoir. The tissue model was

incubated at standard conditions for two hours to allow monocytes to migrate into the collagen matrix. To count the number of monocytes that migrated into the collagen matrix, media in the top and bottom reservoirs were removed, and 4% paraformaldehyde in PBS was added into the tissue models to immobilize the monocytes. The number of monocytes in the collagen matrix was counted in five fields of view, using a light microscope.

To confirm the chemotactic effect of MCP-1 on monocyte migration, the transmigration assay was also performed on a membrane well without the collagen matrix (**Figure 4.1*B***). Complete medium containing monocytes was added to the top reservoir (or the insert) of the membrane well at the same density as described previously, and a 50-ng/mL MCP-1 solution in complete medium was added to the bottom reservoir. For the control samples, complete medium without MCP-1 was added to the bottom reservoir. The membrane wells were incubated for two hours at standard conditions. After the incubation, the top reservoir was removed and the number of monocytes that migrated across the membrane into the bottom reservoir was counted by using a hemocytometer.

ELISA

MCP-1 ELISA was performed as instructed in the manufacturer's manual, except that complete medium was used as diluents for standards and samples instead of Assay Diluent. The plates were assayed on an Emax precision microplate reader (Molecular Devices, Sunnyvale, CA) at the 450 nm wavelength subtracted by the 540 nm reference

wavelength. MCP-1 concentrations were determined by comparing absorbance readings to a standard curve developed from the same assay.

Statistical analysis

Experimental results are expressed as mean ± SD of five samples. For the results of the transmigration assay, student's *t* test was selected to determine a significant difference between the numbers of monocytes migrated into normal and pre-treated collagen matrix. A value of $p < 0.05$ was considered significant.

Results:

Binding reaction between MCP-1 and collagen

To verify the binding reaction between MCP-1 and collagen, media that were collected from the top and bottom reservoirs of the 3D tissue model after pre-treatment with 50-ng/mL MCP-1 solution and after each successive washing step were analyzed for the level of MCP-1. The concentration of MCP-1 measured for each sample is presented in **Table 4.1**. Based on these concentration data, the amounts of MCP-1 in the collagen matrix of the tissue model at the end of the 24-hour incubation and each washing step were estimated. The calculated results show that after 24 hours of incubation, more than 40% of the MCP-1 that was originally added to the tissue model, remained in the collagen matrix (**Table 4.2**). The volume of the collagen matrix is calculated by considering the thickness of the collagen matrix to be 0.37 ± 0.06 mm (measured by using a light microscope at the center area of the matrix) and the cross-sectional area of a membrane insert to be 33 mm^2 (given by the manufacturer). The volume measurement is used to determine the average concentration of MCP-1 in the collagen matrix at this time

point, which is 180 ng/mL. This concentration is nearly four times higher than the initial concentration of MCP-1 solution added into the tissue model and cannot be achieved if diffusion is the only mechanism that controls the distribution of MCP-1 in the system. Thus, there must be a mechanism or reaction that captures MCP-1 inside the collagen matrix. Moreover, such a mechanism appears to strongly confine MCP-1 within the matrix as a very small portion of MCP-1 was recovered after three extensive washes. These findings help support our hypothesis that soluble MCP-1 does bind with collagen to form a static MCP-1 gradient, and that the binding reaction is irreversible.

Table 4.1 The concentration of MCP-1 in the top and bottom reservoirs of the simplified 3D tissue model during the pre-treatment process.

	MCP-1 concentration (ng/mL)
After 24 hours of incubation	
Top medium	5.23 ± 0.67
Bottom medium	3.55 ± 0.06
At the end of the first wash	
Top medium	0.274 ± 0.028
Bottom medium	0.077 ± 0.003
At the end of the second wash	
Top medium	0.057 ± 0.012
Bottom medium	0.009 ± 0.001
At the end of the third wash	
Top medium	< 0.008
Bottom medium	≈ 0

Values are presented as mean ± SD.

Table 4.2 The distribution of MCP-1 in each compartment of the simplified 3D tissue model during the pre-treatment process.

	Amount of MCP-1 (ng)
Initially	
Top medium	5
Bottom medium	0
Collagen matrix	0
After 24 hours of incubation	
Top medium	0.52
Bottom medium	2.31
Collagen matrix (estimated)	2.17
At the end of the first wash	
Top medium	0.027
Bottom medium	0.050
Collagen matrix (estimated)	2.10
At the end of the second wash	
Top medium	0.006
Bottom medium	0.006
Collagen matrix (estimated)	2.08
At the end of the third wash	
Top medium	< 0.001
Bottom medium	≈ 0
Collagen matrix (estimated)	≈ 2.08

Migration assay

It was further hypothesized that if the binding reaction between MCP-1 and collagen does occur, then the concentration gradient of a MCP-1-binding site complex, which is a non-soluble product of the reaction, should have the same meditative effect on monocyte migration as the soluble gradient of MCP-1. To test this assumption, monocytes were added to the top reservoir of the tissue model that was either pre-treated with MCP-1 or without MCP-1, and were allowed to migrate into the collagen matrix for two hours. The percent of monocytes that migrated into the collagen matrix is displayed in **Table 4.3**. Data show that the number of monocytes that migrated into the collagen matrix increases significantly when the collagen matrix was pre-treated with 50-ng/mL MCP-1 solution, compared to when it was not. This finding further supports our hypothesis that the MCP-1 binding reaction and the static MCP-1 concentration gradient, which is caused by the reaction, do exist. Moreover, it demonstrates that the static gradient of MCP-1 can induce monocyte trafficking.

In order to verify the chemotactic effect of MCP-1, the migration of monocytes in response to the soluble concentration gradient of MCP-1 was tested using a membrane well. It was found that the presence of the soluble gradient of MCP-1 across the membrane of the testing system increased the migration of monocytes into the bottom reservoir by almost four times, compared to when there is no MCP-1 added into the system (**Table 4.3**). This result confirms that MCP-1 stimulates chemotaxis of monocytes. Furthermore, when compared to the increase in the migration of monocytes in response to the static gradient of MCP-1, which is about 1.3 times, it suggests that the soluble gradient of MCP-1 might have a stronger effect on the migration of monocytes

than the static gradient does. However, the effect of the static gradient on monocyte migration also takes into account the migration into a collagen matrix; whereas, the soluble gradient does not.

Table 4.3 The percent of monocytes that migrated across the membrane of a membrane well or into the collagen matrix of the simplified 3D tissue model.

	Monocyte migration (%)
Across polycarbonate membrane: (for a membrane well without collagen matrix)	
When the bottom reservoir was filled with complete medium	≤ 1.8
When the bottom reservoir was filled with 50-ng/mL MCP-1 solution	7.2 ± 3.0
Into collagen matrix: (for the 3D tissue model with collagen matrix)	
When the collagen matrix is not pre-treated	23.1 ± 3.0
When the collagen matrix is pre-treated with 50-ng/mL MCP-1 solution	30.3 ± 3.7 **

Values are presented as mean ± SD of the percent of migrated monocytes to the initial numbers of monocytes added to the systems, ** $p < 0.01$ for change in %monocyte migration when the collagen matrix of the tissue model was pre-treated with MCP-1 compared to when the matrix was not pre-treated.

Discussion:

Monocyte trafficking from the bloodstream, across the endothelium, and into a lesion prone area is one of the key elements during the early stage of atherosclerosis. It is believed that the migration of monocytes is promoted by the soluble concentration gradient of MCP-1. However, the understanding about the formation of such gradient in subendothelial matrix is still limited. In our recent study, we found that MCP-1 should be able to bind with collagen, which is a protein that is commonly found in the ECM. This discovery gives rise to a question that *in vivo*, the soluble gradient of MCP-1 may not be the only factor that attracts monocytes into the subendothelial matrix, but the static gradient of the same chemokine may play a role in the recruitment of monocytes as well.

In this current study, we confirmed our finding about the binding reaction between MCP-1 and collagen. Results show that the combined amount of MCP-1 found in the top and bottom reservoirs of the 3D tissue model, after 24 hours of the addition of MCP-1, is only 60% of the initial amount that was added to the model. This finding is similar to what we observed when we examined the formation of MCP-1 concentration gradient using the same tissue model (Manuscript in review). It was also demonstrated that MCP-1 is stable in standard conditions for more than 24 hours, and that there is no significant loss of MCP-1 during the short term storage (less than four days) of samples before they were analyzed (Manuscripts in review). Thus, it is reasonable to believe that the rest of MCP-1 remains in the tissue model and that it should localize in the collagen matrix of the model. However, if all 40% of MCP-1 that resides in the collagen matrix is in a soluble form, then the concentration of MCP-1 in the matrix will exceed the initial concentration of the MCP-1 solution that was added into the tissue model. This is not

possible unless there is a reaction occurring inside the collagen matrix, which consumes MCP-1 and changes it to other forms. We concluded that this reaction should be the binding reaction between MCP-1 and collagen. The binding reaction consumes soluble MCP-1 and converts it into a static product. Based on the evidence found in a study by Distler et al. [29], we also proposed that the binding reaction between MCP-1 and collagen is irreversible. This proposal was supported indirectly by the results of this study, which show that a very small amount of MCP-1 is recovered from the collagen matrix even after extensive washes.

In order to verify the existence of the binding reaction directly, we attempted to measure the concentration of MCP-1 in the collagen matrix. The matrix was pre-treated with MCP-1 solution, to allow the binding between MCP-1 and collagen to occur, and washed extensively to remove any soluble MCP-1 from the matrix. The collagen matrix was digested by using collagenase (Collagenase D – Roche Applied Science; Indianapolis, IN). The amount of MCP-1 in the digested collagen was measured by ELISA. Results reveal that no MCP-1 was detected in the digested collagen (data are not shown). This finding could be due to when MCP-1 binds to collagen, the binding reaction may cause a conformational change to the MCP-1 molecule and thus making it undetectable by the antibodies used in the MCP-1 ELISA.

Another method, though indirect, to validate the presence of the binding reaction between MCP-1 and collagen is to compare the migration of monocytes into the collagen matrix pre-treated with MCP-1 to the collagen matrix not pre-treated with MCP-1. We believed that if MCP-1 does bind with collagen, then the concentration gradient of a MCP-1-binding site complex, which is a product of the binding reaction, should be

created inside the collagen matrix. Since MCP-1 is a chemoattractant for monocytes, and its soluble or chemotactic gradient has a meditative effect on monocyte migration [13, 14, 50-52], then the gradient of static MCP-1 (or the MCP-1-binding site complex) should induce the migration of monocytes as well. It was found in this study that the number of monocytes that migrate into the collagen matrix increases significantly when the matrix is pre-treated with MCP-1. This finding not only helps confirm that the binding reaction does exist, but also proves that monocyte trafficking can be directed by the static or haptotactic gradient of MCP-1.

An additional transmigration assay was performed to demonstrate the effect of a MCP-1 soluble gradient on monocyte migration. Results show that the soluble gradient of MCP-1, which was caused by adding MCP-1 solution to the bottom reservoir of a membrane well, increases the migration of monocytes across the membrane. This is consistent with results from other studies that used similar systems to examine the effect of a soluble gradient of MCP-1 [50-52]. The mechanism in which the soluble gradient of MCP-1 stimulates monocyte migration was proven to be chemotactic, rather than chemokinetic [13, 50].

To determine the different between the migratory effect of chemotactic and haptotactic gradients of MCP-1, results of the transmigration assay in the membrane well were compared to the one tested in the 3D tissue model. Even though we estimated that the average concentration of MCP-1 in the collagen matrix of the tissue model is four times higher than the concentration of MCP-1 solution that was added into the membrane well, we found that the increased number of migrated monocytes, due to the presence of

the MCP-1 gradient, is higher in the membrane well (≈350%) than in the tissue model (≈30%). There are two possible reasons to explain this finding.

First, based on the results of the mathematical model that was developed in our previous study to determine the concentration profile of MCP-1 in the collagen matrix of the tissue model, most of MCP-1 in the collagen matrix is presented in the a static form (Manuscript in review). (These results agree with the findings in this study, which demonstrate that very little soluble MCP-1 can be recovered from the collagen matrix that is pre-treated with MCP-1 solution.) Moreover, several washes were also done to ensure that soluble MCP-1 was completely removed from the collagen matrix before the transmigration assay was performed. Since the binding reaction between MCP-1 and collagen is irreversible, static MCP-1 does not change back to soluble MCP-1. As a result, the static gradient of MCP-1 in the tissue model remains only in the collagen matrix. This allows only monocytes in the top reservoir of the tissue model that are close to the matrix to react with the static gradient of MCP-1 in the matrix. To the contrary, the soluble gradient of MCP-1 is present throughout the top reservoir of the membrane well, due to diffusion of the soluble MCP-1. Thus, more monocytes can react to the gradient of MCP-1 in the membrane well.

Second, for the static gradient of MCP-1 in the tissue model, the results of the mathematical model show that the concentration of static MCP-1 is highest at the top surface of the collagen matrix. Since the migration of monocytes is in response to the positive gradient of MCP-1, monocytes that migrate into the collagen matrix are expected to stay in the area adjacent to the top surface of the matrix. Once there become too many monocytes localized in that area, they may hinder the migration of other monocytes from

the top reservoir of the tissue model into the matrix. This is different than what happens in the membrane well, where monocytes that migrate into the bottom reservoir of the well can move freely because there is no concentration gradient of MCP-1 in the reservoir. Thus, monocytes are more uniformly distributed in the bottom reservoir of the membrane well than in the collagen matrix of the tissue model and do not interfere with the migration across the membrane of other monocytes.

Due to the aforementioned reasons, the causes of the difference between the chemotactic and haptotactic effects of MCP-1 that we observed in this study are believed to be affected by the characteristic (the first reason) and the pattern (the second reason) of each gradient. We cannot determine at this point whether the chemotactic or haptotactic gradients of MCP-1 is more favorable to monocytes, since there are several factors – including the pattern of MCP-1 concentration gradient, and the amount and concentration of MCP-1 in the system – that may affect the migration of monocytes, but are difficult to control. From these initial studies, we suspect that the soluble gradient of MCP-1 may have a greater chemotactic effect; however, the static gradient of MCP-1 may be responsible for attracting a high density of monocytes just below the endothelium, resulting in the site of atherosclerotic plaque formation.

In conclusion, the formation of the static concentration gradient of MCP-1 in the collagen matrix of the 3D tissue model and its haptotactic effect on monocyte migration were examined in this study. Experimental results show there is an irreversible binding reaction between MCP-1 and collagen. Moreover, we demonstrated that static MCP-1, which is a product of the binding reaction, is a chemoattractant to monocytes, but may be less than that of the soluble MCP-1 gradient.

CHAPTER V

CONCLUSIONS AND RECOMMENDATIONS

Conclusions:

This research project focused on the formation of MCP-1 concentration gradients in the collagen matrix of the 3D *in vitro* vascular tissue model. The scope of the project included (1) the examination of the stability of recombinant human MCP-1 under standard cell culture (37°C, humidified atmosphere of 95% air and 5% CO_2) and storage (4°C, -20°C, and -81°C) conditions, (2) the investigation of the binding reaction between MCP-1 and collagen in the matrix, (3) the development of a mathematical model to predict the concentration profiles of MCP-1 in the collagen matrix, and (4) the exploration of the effect of a static MCP-1 concentration gradient on the migration of monocytes. Conclusions are summarized as the following.

i. Recombinant human MCP-1 maintains high stability under standard cell culture conditions in medium that contains at least 10% fetal bovine serum (FBS). The recombinant MCP-1 can be incubated at cell culture conditions without any significant loss for at least seven days.

ii. When stored at non-freezing conditions (4°C), samples containing recombinant human MCP-1 and 10% FBS are stable for at least seven days. However, if the samples are stored at freezing conditions (-20°C or -81°C), then the storage time, MCP-1 concentration of the samples, and the number of freeze-thaw cycles are factors that affect the stability of MCP-1.

iii. The binding reaction between MCP-1 and collagen matrix of the 3D tissue model does occur and it is irreversible. In this binding reaction, soluble MCP-1 is consumed and changed into static MCP-1. As a result, the static concentration gradient of MCP-1 is also created in the collagen matrix.

iv. The developed mathematical model is capable of predicting the concentration of both soluble and static MCP-1 in the collagen matrix of the 3D tissue model within the first 24 hours, when the initial concentration of MCP-1 in the top reservoir is between 5 ng/mL to 50 ng/mL. The overall deviation of the mathematical model is estimated to be approximately 20%.

v. The static concentration gradient of MCP-1 induces the migration of monocytes into the collagen matrix of the 3D tissue model. Compared to the soluble gradient of MCP-1, this static gradient appears to have a weaker effect on monocytes. However, there are differences between the systems that were used to study the effects of the two gradients. Thus, further investigation should be done to confirm this finding.

Recommendations for future studies:

The goal of developing the mathematical model was to estimate the concentration gradients of MCP-1 in the collagen matrix of the 3D tissue model. Although a layer of endothelial cells is neglected in this project in order to reduce the complexity of the mathematical model, eventually the cells need to be included as the source of MCP-1. The followings recommendations are for applying the current mathematical model to the 3D tissue model with a layer of endothelial cells, as well as several suggestions to improve or confirm the results of the current research project.

i. The stability of MCP-1 that is secreted from endothelial cells under cell culture and storing conditions needs to be evaluated, due to other substances secreted by the cells may affect the degradation of MCP-1.

ii. Since MCP-1 will not be initially added to the 3D tissue model, but produced by endothelial cells, the rate of MCP-1 secreted by the cells needs to be determined. An experiment to evaluate MCP-1 secretion includes first growing endothelial cells in the tissue model until they are confluent and stimulating them with an inflammatory factor to mimic inflammatory conditions, i.e. tumor necrosis factor-α. Next, collecting samples from cell culture supernatant at different time points and measuring the concentration of MCP-1. Finally, determining the rate of MCP-1 secretion by using the analytical results.

iii. When applying the rate of MCP-1 secretion to the mathematical model, an additional assumption includes that MCP-1 secreted from the endothelial cells will be well mixed in the top reservoir of the 3D tissue model before diffuses into the collagen matrix. With this assumption, the present mathematical model can

be used, with minimal adjustment to the Excel-VBA program that was used to numerically solve the model. If results from this assumption are not satisfied, then a more complex form of the model must be used.

iv. In order to further verify the existence of static MCP-1 in the collagen matrix, the concentration of MCP-1 should be experimentally determined. Initial studies to measure the average concentration of static MCP-1 in the collagen matrix directly by using ELISA could not detect MCP-1. However, this may not be the best method to measure the concentration of MCP-1 that binds to collagen because the binding may cause some changes to the molecule of MCP-1, preventing it from being recognized by the capture and detection antibodies used in the ELISA. Another way to directly verify the existence of static MCP-1 is to utilize the use of chromatography methods to determine the amount of MCP-1 left in the pre-treated collagen matrix after extensive washes.

v. One way to compare the effect of soluble and static concentration gradients of MCP-1 on monocyte migration is to examine the migration of monocytes into the 3D tissue model containing both types of concentration gradients and compare to the migration of monocytes into the 3D tissue model with just the static concentration gradient. The 3D tissue model with both the soluble and static concentration gradients consists of a pre-treated collagen matrix without any prior washing. This will give a general idea of how the addition of MCP-1 soluble gradient into the system with the static gradient will affect the migration of monocytes.

REFERENCES

1. Scarborough, P., et al. *CVD mortality in Europe*. March 11, 2008 [cited June 3], 2010; Available from: http://www.heartstats.org.
2. *Heart Disease and Strokes Statistics - 2010 Update*. 2010, American Heart Association: Dallas, TX.
3. *Heart Disease and Stroke Prevention: Addressing the National's Leading Killers - 2010 Update*. 2010, Centers for Disease Control and Prevention, National Center for Chronic Disease Prevention and Health Promotion: Altanta, GA.
4. Lusis, A.J., *Atherosclerosis.* Nature, 2000. **407**(6801): p. 233-41.
5. Hansson, G.K., A.K. Robertson, and C. Soderberg-Naucler, *Inflammation and atherosclerosis.* Annu Rev Pathol, 2006. **1**: p. 297-329.
6. Ross, R., *Atherosclerosis--an inflammatory disease.* N Engl J Med, 1999. **340**(2): p. 115-26.
7. Libby, P., *Inflammation in atherosclerosis.* Nature, 2002. **420**(6917): p. 868-74.
8. Vanepps, J.S. and D.A. Vorp, *Mechano-pathobiology of atherogenesis: a review.* J Surg Res, 2007. **142**(1): p. 202-17.
9. Quinn, M.T., et al., *Oxidatively modified low density lipoproteins: a potential role in recruitment and retention of monocyte/macrophages during atherogenesis.* Proc Natl Acad Sci U S A, 1987. **84**(9): p. 2995-8.
10. Ley, K., et al., *Getting to the site of inflammation: the leukocyte adhesion cascade updated.* Nat Rev Immunol, 2007. **7**(9): p. 678-89.
11. Koenen, R.R. and C. Weber, *Therapeutic targeting of chemokine interactions in atherosclerosis.* Nat Rev Drug Discov, 2010. **9**(2): p. 141-53.
12. Gerard, C. and B.J. Rollins, *Chemokines and disease.* Nat Immunol, 2001. **2**(2): p. 108-15.
13. Randolph, G.J. and M.B. Furie, *A soluble gradient of endogenous monocyte chemoattractant protein-1 promotes the transendothelial migration of monocytes in vitro.* J Immunol, 1995. **155**(7): p. 3610-8.
14. Douglas, M.S., et al., *Endothelial production of MCP-1: modulation by heparin and consequences for mononuclear cell activation.* Immunology, 1997. **92**(4): p. 512-8.

15. Wain, J.H., J.A. Kirby, and S. Ali, *Leucocyte chemotaxis: Examination of mitogen-activated protein kinase and phosphoinositide 3-kinase activation by Monocyte Chemoattractant Proteins-1, -2, -3 and -4.* Clin Exp Immunol, 2002. **127**(3): p. 436-44.
16. Newby, A.C., *An overview of the vascular response to injury: a tribute to the late Russell Ross.* Toxicol Lett, 2000. **112-113**: p. 519-29.
17. Ross, R., *The pathogenesis of atherosclerosis: a perspective for the 1990s.* Nature, 1993. **362**(6423): p. 801-9.
18. Napoli, C., et al., *Fatty streak formation occurs in human fetal aortas and is greatly enhanced by maternal hypercholesterolemia. Intimal accumulation of low density lipoprotein and its oxidation precede monocyte recruitment into early atherosclerotic lesions.* J Clin Invest, 1997. **100**(11): p. 2680-90.
19. Navab, M., et al., *The Yin and Yang of oxidation in the development of the fatty streak. A review based on the 1994 George Lyman Duff Memorial Lecture.* Arterioscler Thromb Vasc Biol, 1996. **16**(7): p. 831-42.
20. Dong, Z.M., et al., *The combined role of P- and E-selectins in atherosclerosis.* J Clin Invest, 1998. **102**(1): p. 145-52.
21. Dong, Z.M., A.A. Brown, and D.D. Wagner, *Prominent role of P-selectin in the development of advanced atherosclerosis in ApoE-deficient mice.* Circulation, 2000. **101**(19): p. 2290-5.
22. Nakashima, Y., et al., *Upregulation of VCAM-1 and ICAM-1 at atherosclerosis-prone sites on the endothelium in the ApoE-deficient mouse.* Arterioscler Thromb Vasc Biol, 1998. **18**(5): p. 842-51.
23. Nelken, N.A., et al., *Monocyte chemoattractant protein-1 in human atheromatous plaques.* J Clin Invest, 1991. **88**(4): p. 1121-7.
24. Yla-Herttuala, S., et al., *Expression of monocyte chemoattractant protein 1 in macrophage-rich areas of human and rabbit atherosclerotic lesions.* Proc Natl Acad Sci U S A, 1991. **88**(12): p. 5252-6.
25. Gu, L., et al., *Absence of monocyte chemoattractant protein-1 reduces atherosclerosis in low density lipoprotein receptor-deficient mice.* Mol Cell, 1998. **2**(2): p. 275-81.
26. Gosling, J., et al., *MCP-1 deficiency reduces susceptibility to atherosclerosis in mice that overexpress human apolipoprotein B.* J Clin Invest, 1999. **103**(6): p. 773-8.
27. Weber, K.S., et al., *Differential immobilization and hierarchical involvement of chemokines in monocyte arrest and transmigration on inflamed endothelium in shear flow.* Eur J Immunol, 1999. **29**(2): p. 700-12.
28. Gappa-Fahlenkamp, H. and A.S. Shukla, *The effect of short-term, high glucose concentration on endothelial cells and leukocytes in a 3D in vitro human vascular tissue model.* In Vitro Cell Dev Biol Anim, 2009. **45**(5-6): p. 234-42.
29. Distler, J.H., et al., *Monocyte chemoattractant protein 1 released from glycosaminoglycans mediates its profibrotic effects in systemic sclerosis via the release of interleukin-4 from T cells.* Arthritis Rheum, 2006. **54**(1): p. 214-25.
30. Weadock, K.S., D. Wolff, and F.H. Silver, *Diffusivity of 125I-labelled macromolecules through collagen: mechanism of diffusion and effect of adsorption.* Biomaterials, 1987. **8**(2): p. 105-12.

31. Zhao, X., et al., *Directed cell migration via chemoattractants released from degradable microspheres.* Biomaterials, 2005. **26**(24): p. 5048-63.
32. Fleury, M.E., K.C. Boardman, and M.A. Swartz, *Autologous morphogen gradients by subtle interstitial flow and matrix interactions.* Biophys J, 2006. **91**(1): p. 113-21.
33. Reape, T.J. and P.H. Groot, *Chemokines and atherosclerosis.* Atherosclerosis, 1999. **147**(2): p. 213-25.
34. Rossi, D. and A. Zlotnik, *The biology of chemokines and their receptors.* Annu Rev Immunol, 2000. **18**: p. 217-42.
35. Fernandez, E.J. and E. Lolis, *Structure, function, and inhibition of chemokines.* Annu Rev Pharmacol Toxicol, 2002. **42**: p. 469-99.
36. Deshmane, S.L., et al., *Monocyte chemoattractant protein-1 (MCP-1): an overview.* J Interferon Cytokine Res, 2009. **29**(6): p. 313-26.
37. Melgarejo, E., et al., *Monocyte chemoattractant protein-1: a key mediator in inflammatory processes.* Int J Biochem Cell Biol, 2009. **41**(5): p. 998-1001.
38. Valente, A.J., et al., *Purification of a monocyte chemotactic factor secreted by nonhuman primate vascular cells in culture.* Biochemistry, 1988. **27**(11): p. 4162-8.
39. Matsushima, K., et al., *Purification and characterization of a novel monocyte chemotactic and activating factor produced by a human myelomonocytic cell line.* J Exp Med, 1989. **169**(4): p. 1485-90.
40. Yoshimura, T., et al., *Purification and amino acid analysis of two human glioma-derived monocyte chemoattractants.* J Exp Med, 1989. **169**(4): p. 1449-59.
41. Rollins, B.J., *Monocyte chemoattractant protein 1: a potential regulator of monocyte recruitment in inflammatory disease.* Mol Med Today, 1996. **2**(5): p. 198-204.
42. Yamamoto, T., et al., *Monocyte chemoattractant protein-1 enhances gene expression and synthesis of matrix metalloproteinase-1 in human fibroblasts by an autocrine IL-1 alpha loop.* J Immunol, 2000. **164**(12): p. 6174-9.
43. Johrer, K., et al., *Transendothelial migration of myeloma cells is increased by tumor necrosis factor (TNF)-alpha via TNF receptor 2 and autocrine up-regulation of MCP-1.* Clin Cancer Res, 2004. **10**(6): p. 1901-10.
44. Lee, Y.R., et al., *MCP-1, a highly expressed chemokine in dengue haemorrhagic fever/dengue shock syndrome patients, may cause permeability change, possibly through reduced tight junctions of vascular endothelium cells.* J Gen Virol, 2006. **87**(Pt 12): p. 3623-30.
45. Lu, Y., et al., *Monocyte chemotactic protein-1 mediates prostate cancer-induced bone resorption.* Cancer Res, 2007. **67**(8): p. 3646-53.
46. Hardy, L.A., et al., *Examination of MCP-1 (CCL2) partitioning and presentation during transendothelial leukocyte migration.* Lab Invest, 2004. **84**(1): p. 81-90.
47. Yoshimura, T., et al., *Human monocyte chemoattractant protein-1 (MCP-1). Full-length cDNA cloning, expression in mitogen-stimulated blood mononuclear leukocytes, and sequence similarity to mouse competence gene JE.* FEBS Lett, 1989. **244**(2): p. 487-93.
48. Cushing, S.D., et al., *Minimally modified low density lipoprotein induces monocyte chemotactic protein 1 in human endothelial cells and smooth muscle cells.* Proc Natl Acad Sci U S A, 1990. **87**(13): p. 5134-8.

49. Takeya, M., et al., *Detection of monocyte chemoattractant protein-1 in human atherosclerotic lesions by an anti-monocyte chemoattractant protein-1 monoclonal antibody.* Hum Pathol, 1993. **24**(5): p. 534-9.
50. Sozzani, S., et al., *The signal transduction pathway involved in the migration induced by a monocyte chemotactic cytokine.* J Immunol, 1991. **147**(7): p. 2215-21.
51. Takeya, M., et al., *Production of monocyte chemoattractant protein-1 by malignant fibrous histiocytoma: relation to the origin of histiocyte-like cells.* Exp Mol Pathol, 1991. **54**(1): p. 61-71.
52. Zoja, C., et al., *Interleukin-1 beta and tumor necrosis factor-alpha induce gene expression and production of leukocyte chemotactic factors, colony-stimulating factors, and interleukin-6 in human mesangial cells.* Am J Pathol, 1991. **138**(4): p. 991-1003.

APPPENDICES

APPENDIX A: DIRIVATION OF THE MATHEMATICAL MODEL

Schematic diagram

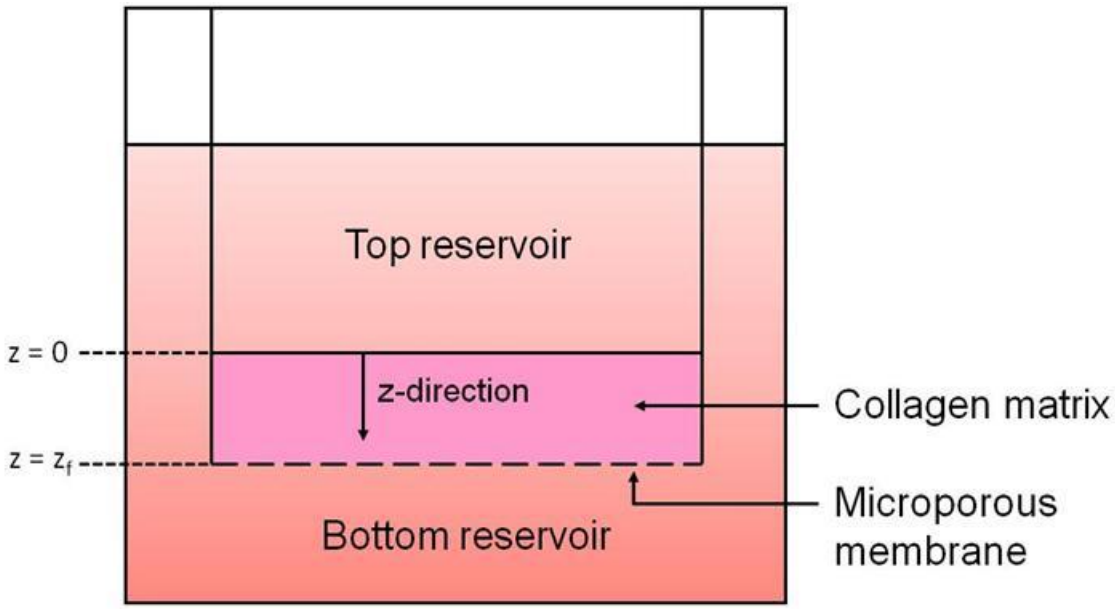

Figure *A*.1 Schematic diagram of a simplified 3D *in vitro* vascular tissue model

List of assumptions

1. There is no convective mass transfer occurring inside the collagen matrix
2. The diffusion of MCP-1 is only in the z-direction.
3. Since the concentration of MCP-1 is very small (in the level of ng/mL or

pmol/mL), the change in the MCP-1 concentration has a negligible effect on the total concentration of the system and, thus, the total concentration is constant.

4. The effective diffusivity of MCP-1 in the collagen matrix is constant.
5. The binding reaction between MCP-1 and collagen is a first-order irreversible reaction, and the rate of reaction depends only on the concentration of MCP-1.
6. MCP-1-binding site ($M{\cdot}S$) complex is a static molecule.
7. The top and bottom reservoirs of the tissue model are well mixed.
8. The MCP-1 concentration at the top surface of the collagen matrix is equal to the concentration of the top reservoir, and the MCP-1 concentration at the bottom surface is equal to the concentration of the bottom reservoir.
9. The volumes of the top and bottom reservoirs are constant.
10. The effect of mass transfer across membrane at the bottom of the collagen matrix, the curvature of the top surface of the collagen matrix, and wall effects are all neglected.

Note: In order to validate assumption #7, the value of the diffusivity coefficient of MCP-1 in the collagen matrix found in this research project was compared to the diffusivity coefficient of MCP-1 in water. Correlations that were used to estimate the diffusivity of MCP-1 in water are similar to those used in the studies of Zhao et al. [31] and Fleury et al. [32]. It was found that the diffusivity of MCP-1 in water is about five to six times higher than the diffusivity of MCP-1 in collagen matrix (values are not shown). This finding suggests that MCP-1 diffuses more quickly in the top and bottom reservoirs than in the collagen matrix. However, since the difference is less than one order of magnitude, further study should be done to confirm that this assumption is valid.

Mass balance equation of MCP-1

Equation of continuity for the mass transfer of MCP-1 in the collagen matrix

$$\frac{\partial C_M}{\partial t} = -\vec{\nabla}\left(c_M \cdot \vec{V}^*\right) - \left(\vec{\nabla} \cdot \vec{\mathrm{J}}_{\mathrm{M}}\right) + R_M \qquad (A.1)$$

① (cancels the convection term)

Rate of change | Rate of convection | Rate of diffusion | Rate of reaction

Apply assumption #1 to equation (*A*.1)

$$\frac{\partial C_M}{\partial t} = -\left(\vec{\nabla} \cdot \vec{\mathrm{J}}_{\mathrm{M}}\right) + R_M \qquad (A.2)$$

Expand the rate of diffusion term using Fick's (first) law of binary diffusion

$$\frac{\partial C_M}{\partial t} = -\left(\frac{\partial\left(-\mathrm{cD_{M|C}}\frac{\partial \mathrm{x_M}}{\partial \mathrm{x}}\right)}{\partial \mathrm{x}} + \frac{\partial\left(-\mathrm{cD_{M|C}}\frac{\partial \mathrm{x_M}}{\partial \mathrm{y}}\right)}{\partial \mathrm{y}} + \frac{\partial\left(-\mathrm{cD_{M|C}}\frac{\partial \mathrm{x_M}}{\partial \mathrm{z}}\right)}{\partial \mathrm{z}}\right) + R_M \qquad (A.3)$$

② ②

Apply assumption #2 to equation (*A*.3)

$$\frac{\partial C_M}{\partial t} = \frac{\partial\left(\mathrm{cD_{M|C}}\frac{\partial \mathrm{x_M}}{\partial \mathrm{z}}\right)}{\partial \mathrm{z}} + R_M \qquad (A.4)$$

Using assumptions #3 and #4, equation (*A*.4) can be rearranged as

$$\frac{\partial C_M}{\partial t} = \mathrm{D_{M|C}}\frac{\partial^2 \mathrm{C_M}}{\partial \mathrm{z}^2} + R_M \qquad (A.5)$$

According to assumption #5, the rate of production of MCP-1 in terms of MCP-1 concentration is

$$R_M = -\mathrm{K_b c_M} \qquad (A.6)$$

Substitute equation (*A*.6) into equation (*A*.5)

$$\boxed{\frac{\partial C_M}{\partial t} = \mathrm{D_{M|C}}\frac{\partial^2 \mathrm{c_M}}{\partial \mathrm{z}^2} - \mathrm{K_b c_M}} \qquad (A.7)$$

Equation (*A*.7) is the mass balance equation of MCP-1 in the collagen matrix.

Mass balance equation of MCP-1-binding site (M·S) complex

Equation of continuity for the mass transfer of *M·S* complex in the collage matrix

$$\frac{\partial C_{M\cdot S}}{\partial t} = -\vec{\nabla}\left(c_{M\cdot S}\cdot \vec{V}^*\right) - \left(\vec{\nabla}\cdot \vec{J}_{\mathrm{M\cdot S}}\right) + R_{M\cdot S} \qquad (A.8)$$

(6) (6)

Rate of change | Rate of convection | Rate of diffusion | Rate of reaction

Apply the assumption #6 to equation (*A*.8)

$$\frac{\partial C_{M\cdot S}}{\partial t} = R_{M\cdot S} \qquad (A.9)$$

The rate of production of the *M·S* complex is equal to the rate of consumption of MCP-1, or

$$R_{M\cdot S} = -R_M = \mathrm{K_b c_M} \qquad (A.10)$$

So, the mass balance equation of the *M·S* complex in the collagen matrix becomes

$$\boxed{\frac{\partial C_{M\cdot S}}{\partial t} = K_b c_M} \qquad (A.11)$$

Boundary conditions

Initially, there is no MCP-1 in the collagen matrix, and the MCP-1 solution is added to the top reservoir of the tissue model. Hence, as suggested by assumptions #7 and #8, the initial conditions for the mass balance equations of MCP-1 and of the *M·S* complex are

$$c_M(z,0) = 0 \tag{A.12}$$

$$c_M(0,0) = c_{i,top} \tag{A.13}$$

$$c_{M\cdot S}(z,0) = 0 \tag{A.14}$$

Two boundary conditions are required for the concentration of MCP-1. They are derived by setting up the mass balance equations of MCP-1 in the top and bottom reservoirs as follows.

Mass balance equation of MCP-1 in the top reservoir

$$Accumulation = In - Out + Generation$$

Because MCP-1 is diffusing from the top reservoir to the bottom reservoir, and since there is no reaction that occurs inside the top reservoir, the 'in' and 'generation' terms are equal to zero. The 'accumulation' term is the molar change of MCP-1in the top reservoir over time. The 'out' term is the rate of MCP-1 transferred into the collagen matrix, which is equal to the rate of diffusion of MCP-1 at the top surface (z = 0) of the collagen matrix.

$$\frac{\partial n_{M,top\ reservoir}}{\partial t} = -A_{top\ surface}\left(\mathrm{J_{Mz}}|_{\mathrm{z=0}}\right) \tag{A.15}$$

Or

$$\frac{\partial\left(c_{M,top\ reservoir}V_{top\ reservoir}\right)}{\partial t} = -A_{top\ surface}\left(\mathrm{J_{Mz}}|_{\mathrm{z=0}}\right) \qquad (A.16)$$

According to assumptions #7 and #8, the concentration of MCP-1 in the top reservoir is equal to the concentration of MCP-1 at the top surface of the collagen matrix.

$$\frac{\partial\left(c_M(0,t)V_{top\ reservoir}\right)}{\partial t} = -A_{top\ surface}\left(\mathrm{J_{Mz}}|_{\mathrm{z=0}}\right) \qquad (A.17)$$

Apply assumption #9 to equation (*A*.17) and rearrange the equation

$$\frac{\partial\left(c_M(0,t)\right)}{\partial t} = -\frac{A_{top\ surface}}{V_{top\ reservoir}}\left(\mathrm{J_{Mz}}|_{\mathrm{z=0}}\right) \qquad (A.18)$$

Expand the rate of diffusion term using Fick's (first) law of binary diffusion and assumption #3

$$\frac{\partial\left(c_M(0,t)\right)}{\partial t} = -\frac{A_{top\ surface}}{V_{top\ reservoir}}\left(-\mathrm{D_{M|C}}\frac{\partial \mathrm{c_M}(0,t)}{\partial \mathrm{z}}\right) \qquad (A.19)$$

Or

$$\boxed{\frac{\partial\left(c_M(0,t)\right)}{\partial t} = \frac{\mathrm{D_{M|C}}A_{top\ surface}}{V_{top\ reservoir}}\left(\frac{\partial \mathrm{c_M}(0,t)}{\partial \mathrm{z}}\right)} \qquad (A.20)$$

The above equation is the top boundary condition of the MCP-1 concentration.

Mass balance equation of MCP-1 in the bottom reservoir

$$Accumulation = In - Out + Generation$$

For the bottom reservoir, the change in MCP-1 concentration is due only to the transport of MCP-1 from the collagen matrix. Thus, the 'out' and 'generation' terms are equal to zero, and the 'in' term is equal to the rate of diffusion of MCP-1 at the bottom surface ($z = z_f$) of the collagen matrix.

$$\frac{\partial n_{M,bottom\ reservoir}}{\partial t} = A_{bottom\ surface}\left(\mathrm{J_{Mz}}|_{\mathrm{z=z_f}}\right) \quad (A.21)$$

Or

$$\frac{\partial\left(c_{M,bottom\ reservoir} V_{bottom\ reservoir}\right)}{\partial t} = A_{bottom\ surface}\left(\mathrm{J_{Mz}}|_{\mathrm{z=z_f}}\right) \quad (A.22)$$

By following the same derivation as demonstrated for the top boundary condition, the final equation for the bottom boundary condition of MCP-1 is

$$\boxed{\frac{\partial\left(c_M(z_f,t)\right)}{\partial t} = -\frac{\mathrm{D_{M|C}} A_{bottom\ surface}}{V_{bottom\ reservoir}}\left(\frac{\partial \mathrm{c_M}(z_f,t)}{\partial \mathrm{z}}\right)} \quad (A.23)$$

Nondimensionalization

In order to simplify the mathematical model and make the values of all variables bound between '0' and '1', nondimiensionalization is performed.

Dimensionless variables

Let $$\varepsilon = \frac{c_M}{c_{i,top}} \quad (A.24)$$

$$\theta = \frac{c_{M\cdot S}}{c_{i,top}} \quad (A.25)$$

$$\tau = \frac{t}{t_f} \quad (A.26)$$

$$\alpha = \frac{z}{z_f} \quad (A.27)$$

Based on the definitions of dimensionless variables (equations (*A*.24-*A*.27)), all variables can be expressed in the form of dimensionless variables as follows.

$$c_M = c_{i,top}\varepsilon, \quad \partial c_M = c_{i,top}\partial\varepsilon, \quad \partial^2 c_M = c_{i,top}\partial^2\varepsilon \quad (A.28)$$

$$c_{M\cdot S} = c_{i,top}\theta, \quad \partial c_{M\cdot S} = c_{i,top}\partial\theta \quad (A.29)$$

$$t = t_f\tau, \quad \partial t = t_f\partial\tau \quad (A.30)$$

$$z = z_f\alpha, \quad \partial z = z_f\partial\alpha, \quad \partial z^2 = z_f^2\partial\alpha^2 \quad (A.31)$$

A nondimensionalized mathematical model is derived by substituting all of expressions (*A*.28-*A*.31) into equations (*A*.7), (*A*.11), (*A*.12-*A*.14), (*A*20), and (*A*23). The following are the nondimensionalized form of the mass balance equations and boundary conditions.

Mass balance equation of MCP-1

$$\frac{\partial \varepsilon}{\partial \tau} = \left(\frac{\mathrm{D_{M|C}t_f}}{\mathrm{z_f^2}}\right)\frac{\partial^2 \varepsilon}{\partial \alpha^2} - \mathrm{K_b t_f}\varepsilon \qquad (A.32)$$

Mass balance equation of MCP-1-binding site (M·S) complex

$$\frac{\partial \theta}{\partial \tau} = K_b t_f \varepsilon \qquad (A.33)$$

Initial conditions

$$\varepsilon(\alpha, 0) = 0 \qquad (A.34)$$

$$\varepsilon(0,0) = 1 \qquad (A.35)$$

$$\theta(\alpha, 0) = 0 \qquad (A.36)$$

Boundary conditions

$$\frac{\partial\left(\varepsilon(0,\tau)\right)}{\partial \tau} = \left(\frac{\mathrm{D_{M|C}t_f}}{z_f} \times \frac{A_{top\ surface}}{V_{top\ reservoir}}\right)\frac{\partial \varepsilon(0,\tau)}{\partial \alpha} \qquad (A.37)$$

$$\frac{\partial\left(\varepsilon(1,\tau)\right)}{\partial \tau} = -\left(\frac{\mathrm{D_{M|C}t_f}}{z_f} \times \frac{A_{bottom\ surface}}{V_{bottom\ reservoir}}\right)\frac{\partial \varepsilon(1,\tau)}{\partial \alpha} \qquad (A.38)$$

Numerical solution

Since the mass balance equation of MCP-1is a linear parabolic PDE, the Crank-Nicolson method was selected to solve the model. An Excel-VBA program was used to solve the mathematical model. To further simplify the problem, an additional assumption, that a "no binding reaction occurs at the top and bottom surface of the collagen matrix", is applied. This assumption adds pseudo boundary conditions for the *M·S* complex to the mathematical model.

$$\theta(0,\tau) = 0 \tag{A.39}$$

$$\theta(1,\tau) = 0 \tag{A.40}$$

It was proven that if the step size in the spatial domain is small enough, then the numerical solution acquired by using this assumption will be similar to when the assumption is not applied (data not shown).

Notation

A = top or bottom surface area of the collagen matrix

α = dimensionless distance from top surface of collagen matrix

c = total molar concentration

$c_{i,top}$ = initial molar concentration of MCP-1in top reservoir

c_M = molar concentration of MCP-1

$c_{M\cdot S}$ = molar concentration of MCP-1-binding site complex

$D_{M|C}$ = effective diffusivity of MCP-1 in collagen matrix

ε = dimensionless concentration of MCP-1

$\vec{J}_M$ = molar flux of MCP-1

J_{Mz} = molar flux of MCP-1 in z-direction

$\vec{J}_{M\cdot S}$ = molar flux of MCP-1-binding site complex

K_b = rate constant of the binding reaction between MCP-1 and collagen

n_M = mole of MCP-1

R_M = molar rate of production of MCP-1

$R_{M\cdot S}$ = molar rate of production of MCP-1-binding site complex

t = time

t_f = final time point

θ = dimensionless concentration of MCP-1-binding site complex

τ = dimensionless time

V = volume of top or bottom reservoir

$\vec{V}^*$ = molar average velocity

x, y, z = Cartesian coordinates

x_M = molar fraction of MCP-1

z_f = thickness of collagen matrix

APPENDIX B: USING AN EXCEL-VBA PROGRAM TO SOLVE THE MATHEMATICAL MODEL NUMERICALLY

An Excel-VBA program, named "Unsteady-state model" was developed and used to find the numerical solution of the mathematical model. The program is divided into two parts. The first part, located in a worksheet called "Main interface", is designed to calculate the concentrations of soluble and static MCP-1 in the collagen matrix of the 3D vascular tissue model at a specified time point. The second part, located in a worksheet called "Parameter regression", is used for performing parameter regression to find the values of the following two unknown constants: (1) the effective diffusivity coefficient of MCP-1 in the collagen matrix ($D_{M|C}$) and (2) the rate constant for the binding reaction between MCP-1 and collagen (K_B). Because the second part is generally used when one runs the program for the first time, the explanation on how to use the program will start from this part.

Parameter regression part

1. Open an Excel file named "Unsteady-state model.xlsm" and select "Parameter regression" worksheet. The parameter regression part of the Excel-VBA program will appear as shown in **Figure *B*.1**.

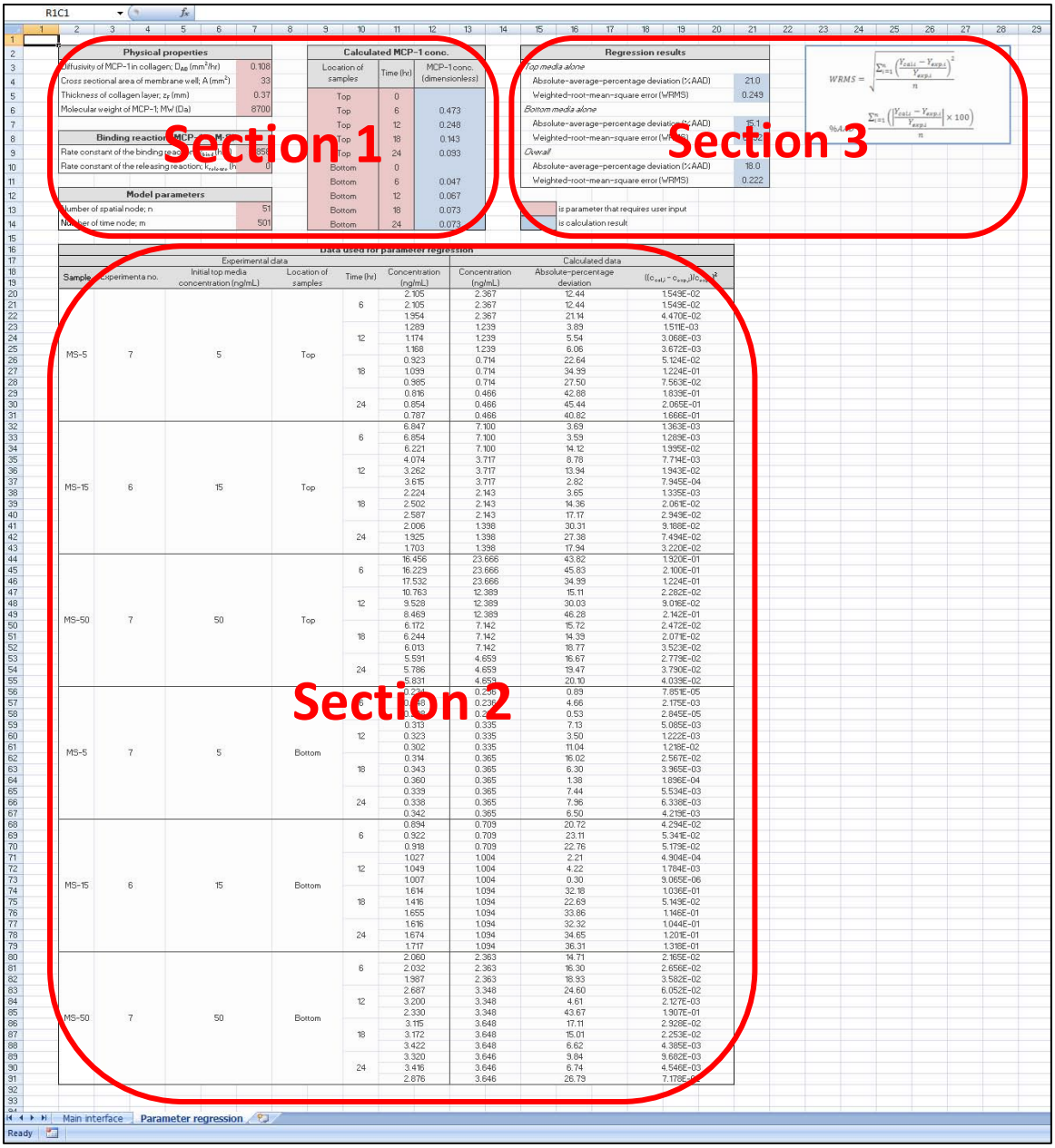

Figure *B*.1 Parameter regression part, showing Sections 1, 2, and 3, of the Excel-VBA program that is designd to solve the mathematical model numerically

2. In Section 1 of the parameter regression part, input the physical properties, rate constants, and model parameters into the highlighted cells, as demonstrated in **Figure *B*.2**.

    2.1. The cross-sectional area of the membrane well is characteristic of the specific type of membrane well, and can be found in the product's technical datasheet.

    2.2. For this research project, the thickness of the collagen layer was approximately 0.37 mm.

    2.3. The molecular weight of MCP-1 is 8.7 kDa.

    2.4. The diffusivity of MCP-1 in collagen ($D_{M|C}$) and the rate constant for the binding reaction (K_B) are the unknown constants being estimated, so the values are initial guesses.

    2.5. Because the binding reaction is irreversible, the rate constant for the releasing reaction (K_R) is zero.

    2.6. The numbers of spatial and time nodes are set by the user. In this research project, they are set to 51 and 501, respectively.

    Note: For this number of spatial node, increasing the number of time nodes beyond 501 has a negligible effect on the regressed results. If more precise results are required, the number of spatial nodes can be increased; however, this will increase calculation time significantly.

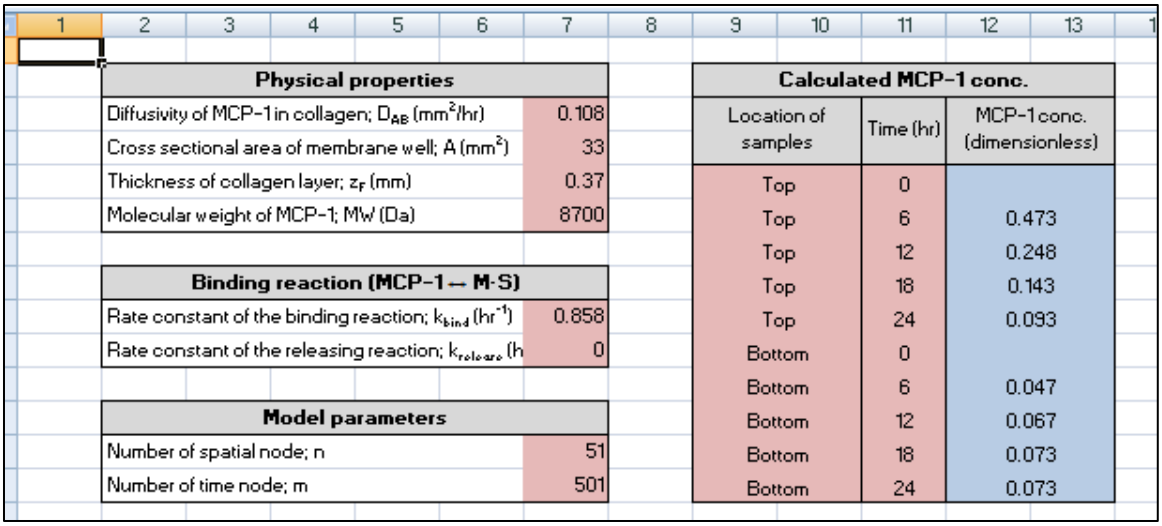

Physical properties	
Diffusivity of MCP-1 in collagen; D_{AB} (mm^2/hr)	0.108
Cross sectional area of membrane well; A (mm^2)	33
Thickness of collagen layer; z_F (mm)	0.37
Molecular weight of MCP-1; MW (Da)	8700

Binding reaction (MCP-1 ↔ M-S)	
Rate constant of the binding reaction; k_{bind} (hr^{-1})	0.858
Rate constant of the releasing reaction; $k_{release}$ (h	0

Model parameters	
Number of spatial node; n	51
Number of time node; m	501

Calculated MCP-1 conc.		
Location of samples	Time (hr)	MCP-1 conc. (dimensionless)
Top	0	
Top	6	0.473
Top	12	0.248
Top	18	0.143
Top	24	0.093
Bottom	0	
Bottom	6	0.047
Bottom	12	0.067
Bottom	18	0.073
Bottom	24	0.073

Figure *B*.2 Section 1 of the parameter regression part. Users need to enter physical properties, rate constants, and model parameters into this section, as well as construct a table to calculate MCP-1 concentrations at locations and time points similar to those of experimental data that are used for performing parameter regression.

3. Also in Section 1, create a table for calculating the dimensionless values of MCP-1 concentration at the specified location and time point.
   3.1. The first column of the table indicates the location of samples, which can be either "Top", or "Bottom" to represent the top reservoir or the bottom reservoir, respectively.
   3.2. The second column indicates the specified time point.
   3.3. The last column is the dimensionless concentration of MCP-1, calculated using the following function: "ConcPR($D_{M|C}$,K_B,K_R,Location,Time)". See in the program for an example of how to use this function.

   Note: For this research project, experimental data used for parameter regression are the concentration of MCP-1 in both the top and bottom reservoirs at time t = 6, 12,

18, and 24 hours. Thus, dimensionless MCP-1 concentrations for the same locations and time points were calculated.

4. In Section 2, create a table containing data used for parameter regression as shown in **Figure *B*.3**.

   4.1. Add experimental data into the "Experimental Data" side of the table as shown in the figure.

   4.2. The values in the column labeled "Concentration" on the "Calculated Data" side of the table are calculated using dimensionless MCP-1 concentration from step 3 and the initial concentration from the "Experimental Data" side of the same table. See in the program for an example of the calculation.

   4.3. Use the same formulas as those in the program to calculate the values in "Absolute-percentage deviation" and "$((c_{cal,i}-c_{exp,i})/c_{exp,i})^2$" columns.

Data used for parameter regression								
Experimental data						Calculated data		
Sample	Experimenta no.	Initial top media concentration (ng/mL)	Location of samples	Time (hr)	Concentration (ng/mL)	Concentration (ng/mL)	Absolute-percentage deviation	$((c_{cal,i}-c_{exp,i})/c_{exp,i})^2$
MS-5	7	5	Top	6	2.105	2.367	12.44	1.549E-02
					2.105	2.367	12.44	1.549E-02
					1.954	2.367	21.14	4.470E-02
				12	1.289	1.239	3.89	1.511E-03
					1.174	1.239	5.54	3.068E-03
					1.168	1.239	6.06	3.672E-03
				18	0.923	0.714	22.64	5.124E-02
					1.099	0.714	34.99	1.224E-01
					0.985	0.714	27.50	7.563E-02
				24	0.816	0.466	42.88	1.839E-01
					0.854	0.466	45.44	2.065E-01
					0.787	0.466	40.82	1.666E-01
MS-15	6	15	Top	6	6.847	7.100	3.69	1.363E-03
					6.854	7.100	3.59	1.289E-03
					6.221	7.100	14.12	1.995E-02
				12	4.074	3.717	8.78	7.714E-03
					3.262	3.717	13.94	1.943E-02
					3.615	3.717	2.82	7.945E-04
				18	2.224	2.143	3.65	1.335E-03
					2.502	2.143	14.36	2.061E-02
					2.587	2.143	17.17	2.949E-02
				24	2.006	1.398	30.31	9.188E-02
					1.925	1.398	27.38	7.494E-02
					1.703	1.398	17.94	3.220E-02

Figure *B*.3 Section 2 of the parameter regression part. Experimental data that are used for performing parameter regression are added into this section. Deviations between experimental and calculated data are also calculated in this section.

5. In Section 3, create a table to contain regression parameters as shown in **Figure *B*.4**. The equations used to calculate the absolute-average-percentage deviation (%AAD) and weighted-root-mean-square error (WRMS) are also displayed in the figure, as well as in the program.

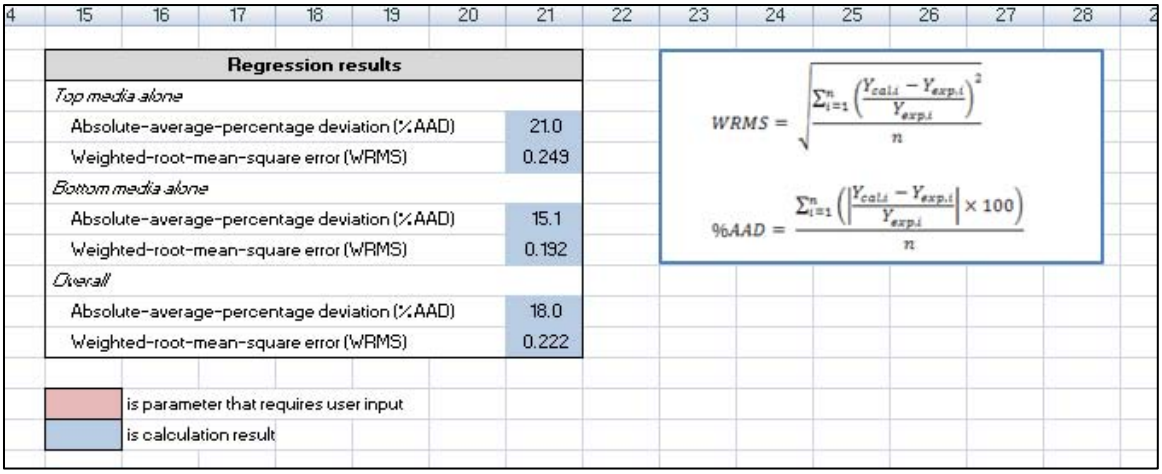

Regression results	
Top media alone	
Absolute-average-percentage deviation (%AAD)	21.0
Weighted-root-mean-square error (WRMS)	0.249
Bottom media alone	
Absolute-average-percentage deviation (%AAD)	15.1
Weighted-root-mean-square error (WRMS)	0.192
Overall	
Absolute-average-percentage deviation (%AAD)	18.0
Weighted-root-mean-square error (WRMS)	0.222

is parameter that requires user input

is calculation result

$$WRMS = \sqrt{\frac{\sum_{i=1}^{n}\left(\frac{Y_{cal,i} - Y_{exp,i}}{Y_{exp,i}}\right)^2}{n}}$$

$$\%AAD = \frac{\sum_{i=1}^{n}\left(\left|\frac{Y_{cal,i} - Y_{exp,i}}{Y_{exp,i}}\right| \times 100\right)}{n}$$

Figure *B*.4 Section 3 of the parameter regression part, showing overall deviation between experimental and calculated data.

6. To perform parameter regression, go to tab “Data” in the Excel menu and select “Solver”.
   6.1. In the solver menu, set the cell that contains overall WRMS to be the target cell.
   6.2. In the next line which begins with “Equal to”, select “Value of” and enter ‘0’ into the box.
   6.3. Set the cells containing the initial guesses for $D_{M|C}$ and K_B to be the changing cells.
   6.4. In the “Subject to the Constraints” box, put in the constraints that limit the values of the changing cells to be equal to or more than zero.

6.5. Click “Solve” button and wait until the solver stops running. This process could take a long time (approximately 4-6 hours).

Note: The Solver function finds the values of $D_{M|C}$ and K_B that give the best fit of the mathematical-model results to the experimental data. (The perfect fit occurs when WRMS is equal to zero).

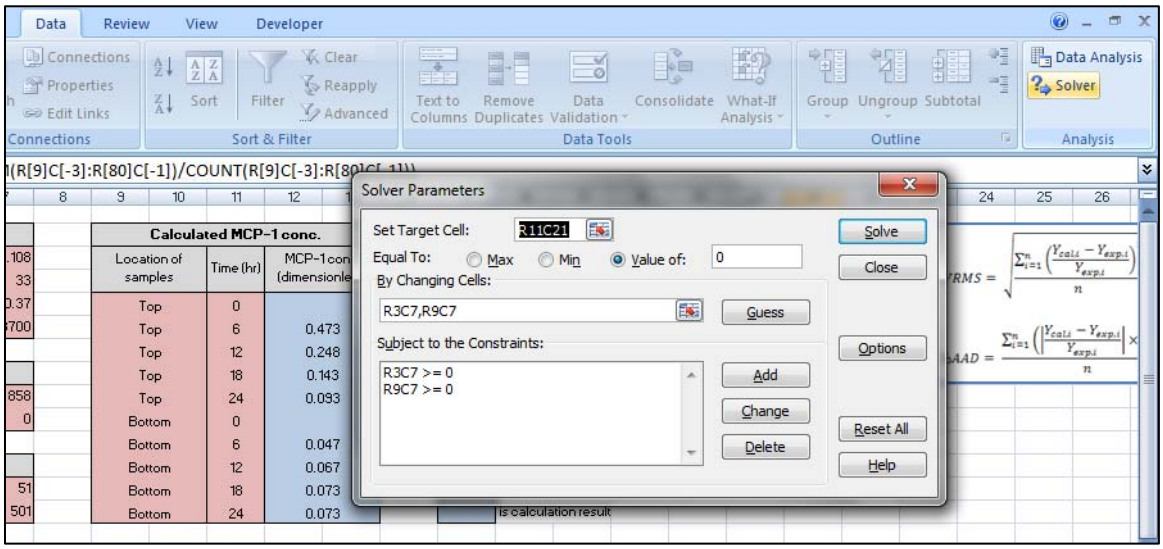

Figure *B*.5 Microsoft Excel 2007 Solver menu

7. Once the Solver function stops running, select the option to keep the new values of $D_{M|C}$ and K_B. The initial guess values that were previously put into the program will be updated to the new values.

Main interface part

1. Open an Excel file named "Unsteady-state model.xlsm" and select "Main interface" worksheet. (Or if the program has already been opened, select "Main interface" worksheet). Main interface part of the Excel-VBA program will appear as shown in **Figure *B*.6**.
2. Click "Clear" button to delete any previous results.
3. Input the physical properties, the rate constants, and the model parameters into the corresponding cells.
   3.1. The values of the regressed $D_{M|C}$ and K_B in the "Parameter regression" worksheet can be copied and pasted into the "Main interface" worksheet by using the "paste values" option.
   3.2. However, when the regressed $D_{M|C}$ and K_B values are used, it is important to make sure that the numbers of spatial and time nodes in the main interface are the same as those used in the parameter regression. This is because the precision of the MCP-1 concentration values calculated from the regressed parameters is tied to the number of nodes used in the calculation.
4. When all of the required values are entered, click the "Calculate" button and wait until the program stops running. The calculated concentrations of both soluble and static MCP-1 for each spatial node at the final time point will be displayed. These values can be copied to other Excel files for further use, such as graphing.
5. If the user needs to find MCP-1 concentrations at other time points, click the "Clear" button to delete the current results, then change the final time point to a new value and click the "Calculate" button again.

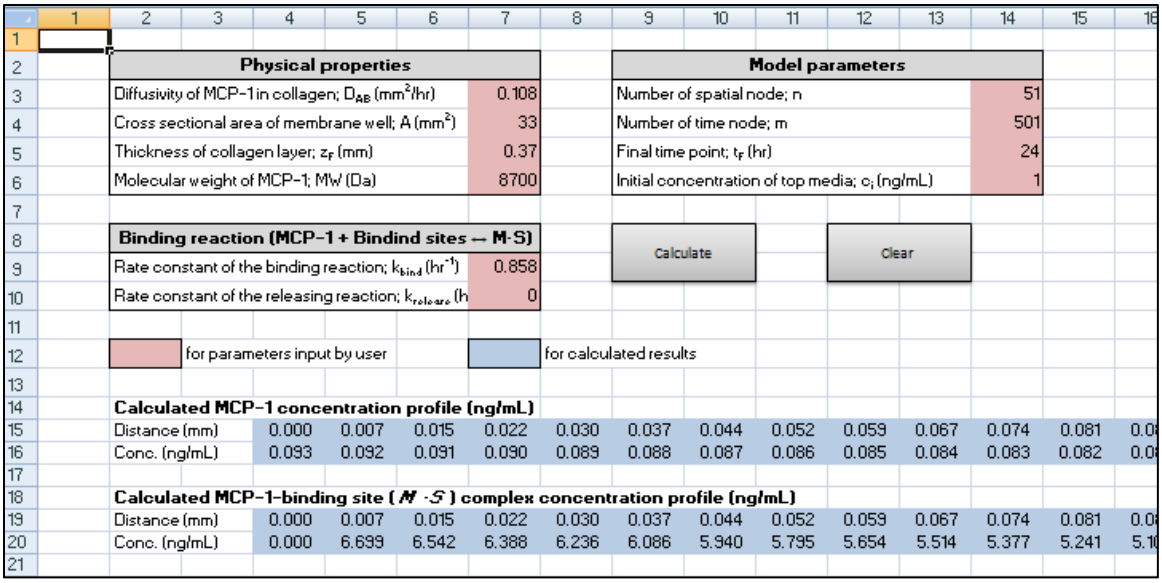

Physical properties		Model parameters	
Diffusivity of MCP-1 in collagen; D_{AB} (mm^2/hr)	0.108	Number of spatial node; n	51
Cross sectional area of membrane well; A (mm^2)	33	Number of time node; m	501
Thickness of collagen layer; z_F (mm)	0.37	Final time point; t_F (hr)	24
Molecular weight of MCP-1; MW (Da)	8700	Initial concentration of top media; c_i (ng/mL)	1

Binding reaction (MCP-1 + Bindind sites ↔ M-S)	
Rate constant of the binding reaction; k_{bind} (hr^{-1})	0.858
Rate constant of the releasing reaction; $k_{release}$ (h	0

Calculate | Clear

for parameters input by user | for calculated results

Calculated MCP-1 concentration profile (ng/mL)													
Distance (mm)	0.000	0.007	0.015	0.022	0.030	0.037	0.044	0.052	0.059	0.067	0.074	0.081	0.0
Conc. (ng/mL)	0.093	0.092	0.091	0.090	0.089	0.088	0.087	0.086	0.085	0.084	0.083	0.082	0.0

Calculated MCP-1-binding site ($\mathcal{M}$-$\mathcal{S}$) complex concentration profile (ng/mL)													
Distance (mm)	0.000	0.007	0.015	0.022	0.030	0.037	0.044	0.052	0.059	0.067	0.074	0.081	0.0
Conc. (ng/mL)	0.000	6.699	6.542	6.388	6.236	6.086	5.940	5.795	5.654	5.514	5.377	5.241	5.1

Figure *B*.6 Main interface part of the Excel-VBA program that is used to solve the mathematical model numerically

VITA

Krisada Leemasawatdigul

Candidate for the Degree of

Master of Science

Thesis: FORMATION OF CONCENTRATION GRADIENTS OF MONOCYTE CHEMOATTRACTANT PROTEIN-1 IN A COLLAGEN MATRIX

Major Field: Chemical Engineering

Biographical:

Education:

Completed the requirements for the Master of Science in Chemical Engineering at Oklahoma State University, Stillwater, Oklahoma in July, 2010.

Completed the requirements for the Bachelor of Engineering in Chemical Engineering at Chulalongkorn University, Bangkok, Thailand in April, 2007.

Experience:

Employed as a graduate research and teaching assistance by Department of Chemical engineering, Oklahoma State University, Stillwater, Oklahoma from August 2008 - present.

Worked as an intern in PTT Chemical Public Company Limited, Rayong, Thailand from March - May 2006.

Name: Krisada Leemasawatdigul Date of Degree: July, 2010

Institution: Oklahoma State University Location: Stillwater, Oklahoma

Title of Study: FORMATION OF CONCENTRATION GRADIENTS OF MONOCYTE CHEMOATTRACTANT PROTEIN-1 IN A COLLAGEN MATRIX

Pages in Study: 86 Candidate for the Degree of Master of Science

Major Field: Chemical Engineering

Scope and Method of Study:

This research project determined the formation of the static and soluble concentration gradients of monocyte chemoattractant protein-1 (MCP-1) in a collagen matrix using a 3D *in vitro* vascular tissue model. Stability of MCP-1 and the binding reaction between MCP-1 and collagen were examined and used to develop a mathematical model to estimate the concentration of MCP-1 within the collagen matrix. Effect of storage conditions on the stability of MCP-1 and the effect of a static gradient of MCP-1 on monocyte migration were also investigated in this project.

Findings and Conclusions:

Recombinant human MCP-1, within a medium containing 10% fetal bovine serum, is stable at standard cell culture conditions (37°C in humidified atmosphere of 5% CO_2 and 95% air) for seven days. However, storage conditions and duration, as well as the concentration of MCP-1, can affect the stability of MCP-1 when it is stored at working concentrations. Also, it was found that binding reaction between MCP-1 and collagen does exist and is irreversible. Based on these findings, a mathematical model to describe the transport of MCP-1 through the collagen matrix was developed. Results from the mathematical model showed that both static and soluble concentration gradients of MCP-1 are formed in the matrix. The static gradient of MCP-1 was proven to have haptostatic effect on monocyte migration. When the pattern of the static gradient of MCP-1 was taken in to account, this latter finding suggests that the static gradient of MCP-1 may be responsible for attracting high density of monocyte just below the endothelium, as observed in the site of atherosclerosis lesions.

ADVISER'S APPROVAL: Dr. Heather Fahlenkamp